VOL.VII No 3 DECEMBER 2010

JMR
JOURNAL OF MARITIME RESEARCH

Spanish Society of Maritime Research

JMR JOURNAL OF MARITIME RESEARCH

VOL. VII N.o3
DECEMBER 2010

JMR
JOURNAL OF MARITIME RESEARCH

UNIVERSITY OF CANTABRIA

Escuela Técnica Superior de Náutica
c/ Gamazo nº1, 39004 SANTANDER
Telfno (942) 201362; Fax (942) 201303
e-mail: info.jmr@unican.es
http://www.jmr.unican.es

Layout: JMR

Printed bay: Gráficas Ebro, S.L.

ISSN: 1697-4840

D. Legal: SA-368-2004

CONTENTS

Journal of Maritime Research, Vol. VII. No. 3, pp. 3-14, 2010

ISSN: 1697-4840

VESSEL CONDITION MONITORIZATION THROUGH SATELLITE USING PRINCIPAL COMPONENT ANALYSIS

J.L. Larrabe[1,2], M.A. Gómez[1,3], I. Sotés[1,2], F.J. Alvarez[1,4], M.C. Rey[1,4], V.E. Mielgo[1,4], I. Sotes[1,2], X. Basogain[1,2]

Received 27 November 2009; in revised form 4 December 2009; accepted 15 August 2010

ABSTRACT

Abstract - Offshore telecommunications are possible in virtually all parts of the world via satellite. Satellite communications are increasing the bandwidth and lowering the cost, but are still far from levels that are in earth. Principal components analysis (PCA) is a statistical technique that has found application in fields such as biometrics or compression of images, being a common tool for the search of pattern of multidimensional data sets. The hypothesis of this study was the possibility of using the PCA theory to compress, with sufficient accuracy, the large amount of data that are collected on board, and then send them all via satellite, in a cheaper and faster way than traditionally. The materials used were 44 samples of 182 different signals, obtained from 19 different equipment on board the LNG vessel "Castillo de Villalba". With these data the PCA algorithm was applied, using a computer program developed by the authors, generating new data packets to send by satellite. Different strategies were used in order to ensure that the correlation coefficient was equal or greater than 0.95 in the comparison between original data and reconstructed data onshore. Results obtained by grouping the 182 signals showed 46.9% reduction in data sent via satellite, with a mean r = 0.95 ± 0.08. This strategy is appropriate for decision making about tele-diagnosis and maintenance of the ship using ground equipment. Consequently, significant savings are achieved in telecommunication costs and telecommunication times.

Keywords: Vessel, telecommunications, satellite, compression, lossy.

[1] Universidad del País Vasco, Tel. 946014847, Fax. 946017700, María Díaz de Haro 68 48920 Portugalete, Spain. [2]Professor, Email: jl.larrabe@ehu.es, [3]Professor, Email: cnpgosom@lg.ehu.es, [4]Researcher, Email: jl.larrabe@ehu.es.

INTRODUCTION

Communications at sea are in the process of evolution. Satellite coverage is practically worldwide for the main marine technologies used today, such as Iridium, Inmarsat, Very Small Aperture Terminal (VSAT), etc. Moreover, much progress is being made in increasing the bandwidth as well as in reducing the required hardware prices and the communications fees. This paper presents a Lossy Compression Technique or data non-exact compression method by applying principal component analysis (PCA). It is proposed for monitoring the condition of equipment on board of surface vessel or underwater vehicles, which allows a lower cost of communication, reducing the used satellite time or bandwidth (Calvo et al. 2009; Gomariz et al. 2009; Horak 2007; Organización, I 2008; Organización, I & Organización de Aviación Civil Internacional (Montreal 2008).

The first part of the introduction shows the main communication systems used in the shipbuilding industry, such as Iridium, Inmarsat and VSAT and bandwidths and prices available for communication are analyzed. Subsequently, we examine the procedures for lossless and lossy data compression, indicating the characteristics of each. Finally, an introduction to the procedure of principal components analysis is done.

The International Convention for the Safety of Life at Sea (SOLAS), adopted under the support of the International Maritime Organization (IMO), an agency of the UN, the implementation on board of the Global Maritime Distress and Safety (GMDSS). It is a set of safety procedures, equipment and communication protocols designed to enhance safety and simplicity of navigation and rescue boats at risk. It is in force at merchant and passenger ships since 1999. The system seeks to carry out the following: to alert, including position determination of the unit in distress, search and rescue coordination, locating the provision of maritime information, general communications and communications bridge to bridge. The network of satellites operated by Inmarsat, under the supervision of the IMO, is a key element of the GMDSS system in order to provide telephony and data services to users worldwide (coverage spans the globe except the polar regions above 70 degrees of latitude), via special terminals which communicate to ground stations through twelve geosynchronous telecommunications satellites. Inmarsat launches into space every few years a new generation of satellites, with increasingly more powerful features. Hardware prices vary between 3,000 and 20,000 Euros, having a variety of types of terminals (Fleet F77, Fleet F55, Inmarsat M, Inmarsat C, Inmarsat B, etc). The newest product line is the Inmarsat BGAN (Broadband Global Area Network) terminals to enable data transmission of up to 432 kbps in terminals ranging from the size of a small notebook and weighing 0.9 kg. The estimated costs of a voice call via the Inmarsat systems are about 1.2 € per minute and the broadband data transmission have an average of 5.4 € per Megabyte. These costs are approximate and vary depending on telecommunication provider (Horak 2007; Organización, I 1995;

Organización, I 2008; Organización, I & Organización de Aviación Civil Internacional (Montreal 2008).

Thanks to the Inmarsat system, vessels and platforms can be communicated around the world to a similar level than land users, although at a higher cost. This is enabling new schemes in the operation of ships, improving security, enabling onboard personnel reduction and optimizing its operation.

Recently, new alternatives have been developed for offshore data transmission, such as the Iridium system and VSAT. Iridium is the name of a communication network which has 66 satellites in total arranged, in 11 longitudinal orbits of 6 satellites each. This network was designed by Satellital Movil Phone Services from Motorola, with global coverage (including the poles) and, it was put on service on 1998. Initially, it was a very expensive service because of the high price of the hardware. For example, an antenna reached 2,700€, and the cost of communication about 5.42 € per minute. Now, Iridium has the OpenPort service directed to maritime market which will be able to transmit up to 128 Kbps worldwide; the cost of the terminal reaches 4,600 € and the transmission –reception data costs will be 3.90 € per Megabyte (Elbert 1999; Elbert 2008; Horak 2007; Organización, I 2008).

VSAT is a data transmission technology between an earth station and a satellite, with directional dish antenna, that is smaller than 3 meters. Data rates typically range from narrowband 54 kbps to more than 18 Mbps. VSATs are used for maritime communications with a special design to withstand tough marine conditions by adjusting antenna position and maintaining lock on the satellite allowing for the ship's motion and turning. VSAT network consists of a constellation of satellites and a terrestrial network. Depending on the chosen frequency coverage is global (C band 3-7 GHz) or Regional (Ku band 12-14 GHz), with all shore coverage and a few miles from the coast. The cost of the terminal is between 45,000 to 200,000 € and the transmission–reception costs are determined by a flat rate in terms of 3,000-15,000 € per month, in agreement to contract for services with the telecommunication operator (Horak 2007; Organización, I 2008). The figure 1 shows an example of comparison of communication costs per month [€] between Iridium Openport, Imarsat FeetBroadBand 500 and VSAT technologies. For large amount of data traffic, VSAT solution is an economical solution.

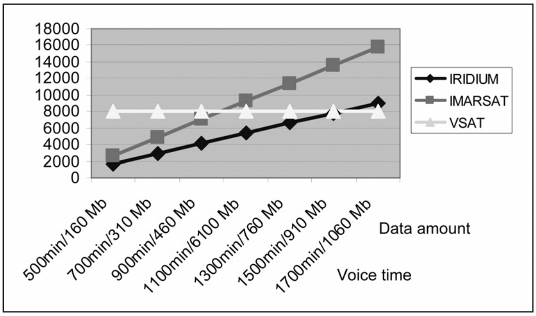

Figure 1. Data transmission from vessel: example of comparison of communication costs per month [€] between Iridium Openport, Imarsat FBB500 and VSAT technologies.

In order to reduce fees of satellite communication at sea, there are two ways to compress information: lossless and lossy way. The lossless compression algorithms usually use statistical redundancy to represent the data without error. The compression methods are possible because most real-world data has statistical redundancy. For example, in English text, the letter 'e' is much more common than the letter 'z', and the probability that the letter 'q' is followed by the letter 'z' is very small.

Another compression technique, called lossy data compression, is possible if some loss of fidelity is acceptable. In general, lossy data compression will be guided by research on how people perceive the data in question. For example, the human eye is more sensitive to subtle variations in brightness than variations in colour. JPEG image compression works, in part, by "rounding off" method to lessen information. Lossy data compression provides a way to obtain better compression rates of a given amount of data. In some cases, data reliability is required and lossy compression will be questioned; in other cases, fidelity can be sacrificed to reduce the amount of data as much as possible (Grailu, Lotfizad, & Sadoghi-Yazdi 2009; Steinberg 2009).

Lossless data compression is reversible, so that the original data can be rebuilt, while lossy data compression accepts some loss of data in order to achieve greater compression. Repeatedly lossy compressing and decompressing the file will cause it to progressively lose quality. Lossy methods are most often used for compressing sound, images or videos. This is because these types of data are intended for human interpretation where the mind can easily "fill in the blanks" or see past very minor errors or inconsistencies. In practice, lossless data compression also gets to a point where compressing again does not work, although lossy extreme algorithms, such as removing the last byte of a file will always compress the file up to the point where it becomes empty.

Principal Component analysis (PCA) is a useful statistical technique that has found application in fields such as face recognition and image compression, and is a common technique for finding patterns in large data (Belogolovy et al. 2009; Johnson, Rose-Pehrsson, & Morris 2004; Prasad 2007; Xiong, Liang, & Qian 2007).

It is a way of identifying patterns in data and expresses it in such a way that highlights their similarities and differences. Because patterns can be difficult to find in data of high dimension, where the luxury of graphical representation is not available, PCA is a powerful tool for data analysis (Lee, Qin, & Lee 2007; Manly 2005; Mason & Young 2002).

The other main advantage of PCA is that once you have found these patterns in the data, you can compress it, reducing the number of dimensions, without much loss of information (Johnson, Rose-Pehrsson, & Morris 2004; Prasad 2007; Xiong, Liang, & Qian 2007).

For this work, the hypothesis was based on the possibility to use the theory of PCA and perform lossy compression of large amounts of collected data by the control system onboard ships and send it via satellite saving time or reducing costs.

OBJECTIVES

1. To develop a computer program for compression and decompression of the algorithms data collected on board using PCA.
2. To find the best strategy to compress data using PCA.

MATERIALS AND METHODS

The data used were collected on board a ship which transported liquefied natural gas LNG (Castillo de Villalba) through its integrated automation system (IAS, Norcontrol, Norway). This device generates a spreadsheet file every 12 hours, which represents the condition of 182 different signals of the 19 major subsystems of the vessel: Main Turbine, Boiler Common, Boiler No. 1 Boiler No 2, Turbo Generator No 1, Turbo Generator No 2, Diesel Generator, Boiler Water Readings, Feed Cond. System, Evaporators, Water Tanks, Fuel Oil, Marine Diesel Oil, Gas Oil, Sludge and Bilge, Others, LD Compressors and Fridges-Air Conditioning.

It was considered a pilot-pilot travel Saint-Nazaire (France) - Bonny (Nigeria) with a duration of 22 days, representing 44 different values for each signal, representing 44 different values for each signal and obtaining data from 8008 double precision floating point (64 bits). The data set keeps the correlations between the signals for the normal operation of the ship: loading, unloading, ballast voyage and travel in cargo. The original data were stored in a matrix called $[Data]_{mxn}$, where the samples or observations were rows (m) and columns (n) were dimensions, previously cited as signals (Torokhti & Friedland 2009).

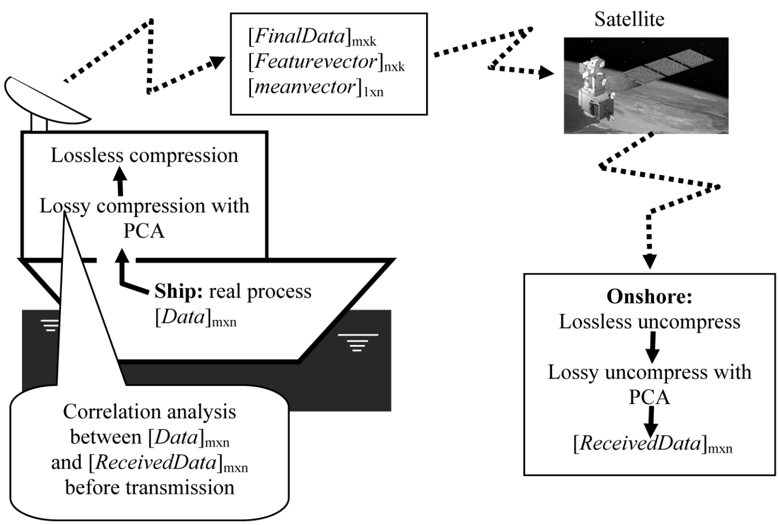

Figure. 2. Block diagram of the transmission method using lossy compression with PCA.

Two computer programs were developed by the authors (Labview 8.2, National Instrument, Austin TX). One of them performs PCA and generated the packets to send by satellite offshore. The second program uncompressed data onshore. All results were displayed graphically and saved in file format compatible with spreadsheet programs. Figure 2 shows the block diagram of the transmission method.

Several steps were given to determine PCA (Lee, Qin, & Lee 2007; Mason & Young 2002; Prasad 2007; Xiong, Liang, & Qian 2007). First, from each dimension, was subtracted the mean. This produced a data set ($[DataAdjust]_{mxn}$) whose mean was zero:

$$DataAdjust_{ij} = Data_{ij} - \overline{\{Data_{xj} \mid x = 1,\dots,m\}} \tag{1}$$

where i was observation, j was dimension and m was total number of observations.

Second the $[covariance\ matrix]_{nxn}$ of $[DataAdjust]_{mxn}$ was evaluated. The eigenvalues λ and eigenvectors $\boldsymbol{x}$ for $[covariance\ matrix]_{nxn}$ were calculated as third step: eigenvalues λ_j were used for calculation of [% of total variance] (V_j) for each component j:

$$V_j = 100 \frac{\lambda_j}{\sum_{x=1}^{n} \lambda_x} \qquad \sum_{x=1}^{n} \lambda_x = n \tag{2}$$

After components were chosen to form feature vector: Eigenvalues λ and eigenvectors $\mathbf{x}$ are sorted in descending order. Component with highest λ was considered principal component and $[Featurevector]_{nxk}=(\mathbf{x}_1, \mathbf{x}_2, \dots, \mathbf{x}_k)$, where $\mathbf{x}_i$ was a column oriented eigenvector, contains chosen components (k).

To derive new dataset was performed the transpose of [*Featurevector*] and [*DataAdjust*] in order to get original data in terms of chosen components:

$$[FinalData^T]_{kxm} = [FeatureVector^T]_{kxn} \ x \ [DataAdjust^T]_{nxm} \tag{3}$$

FinalData has eigenvectors as coordinate axes.

After choosing proper components, was prepared the package of double precision numbers (64 bit) to send once for satellite:

$$\begin{aligned} &[FinalData]_{mxk} \\ &[Featurevector]_{nxk} \\ &[meanvector]_{1xn} \end{aligned} \tag{4}$$

These data were received on shore and the procedure of reconstruction of the data settles down in destination:

$$[ReceivedData]_{mxn} = ([Featurevector]_{nxk} \ x \ [FinalData^T]_{kxm})^T + [meanvector]_{mxn} \quad (5)$$

having $[meanvector]_{mxn}$ matrix all m rows equal to $[meanvector]_{1xn}$. This procedure yields original data using the chosen components (figure 2).

Simplifying for not going into details of programming, the designed computer application chosen in sequence the eigenvectors from highest to lowest eigenvalue and calculated the mean *r* correlation coefficient of all the variables from the matrix with the real data $[Data]_{mxn}$ and the received matrix $[ReceivedData]_{mxn}$. When *r* was greater or equal than a given threshold, the data package to send was prepared. In the case of this work, the threshold chosen was $r \geq 0.95$. The figure 3 shows the front panel of that program (Khoo 2000; Peña Sánchez de Rivera 1995).

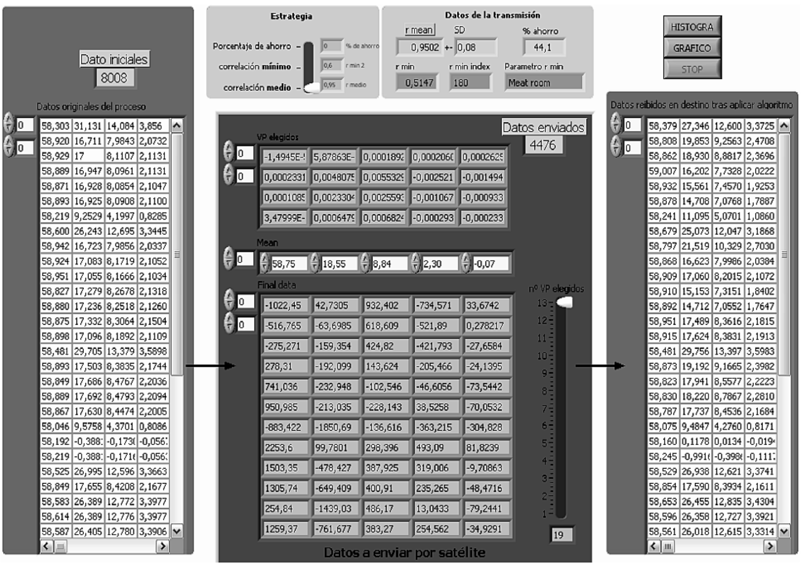

Figure 3. Front panel of the designed computer application. In the left side are the real data collected onboard. In the centre are the three packets sent by satellite. In the right side it is shown received data.

Two methods were analyzed: on the one hand all 182 signals were compressed together (table 1) and only one packet to be sent was created. On the other hand each vessel subsystem was treated independently, i.e. 34 signal of main turbine, 12 signals of Boiler nº 1, etc. (table 2). Now 19 different packets were created to be send. In all cases the following items were evaluated: number of principal components used, coefficient of correlation, number of original data, number of sent data and file space saved taking into account that each value needed 64 bits for its representation. The Histogram of coefficient of correlation *r* obtained sending all collected onboard variables (182) and separately are shoed in the figure 4 and 5.

RESULTS

	Number of Signals	Number of principal components used	Coefficient correlation	Number of original data	Number of sent data	File space saved
All equipments together	182	18	0.95±0.08	8008	4250	46.9%

Table 1. Obtained transmision results sending all collected onboard variables together.

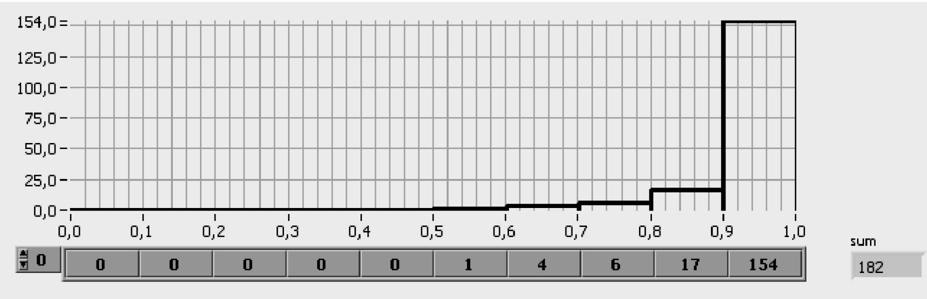

Figure 4. Histogram of coefficient of correlation *r* obtained sending all collected onboard variables (182) together. 154 (84.6 %) of them presented *r* between 0.9 and 1. All signal presented *r* > 0.5.

		Number of Signals	Number of principal components used	Coefficient correlation	Number of original data	Number of sent data	File space saved
1	Main Turbine	34	6	0.95±0.11	1496	502	66.4 %
2	Boiler Common A	4	4	1±0	176	196	-11.4 %
3	Boiler Common B	3	2	1±0	132	97	26.5 %
4	Boiler nº1	12	6	0.96±0.09	528	348	34.1 %
5	Boiler nº2	12	7	0.95±0.11	528	404	23.5 %
6	Turbo Generator No 1	12	2	0.97±0.04	528	124	76.5 %
7	Turbo Generator No 2	12	3	0.99±0.02	528	180	65.9 %
8	Diesel Generator	17	2	0.97±0.08	748	139	81.4 %
9	Boiler Water Readings	4	4	1±0	176	196	-11.4%
10	Feed Cond. System	12	7	0.95±0.12	528	404	23.5 %
11	Evaporators	2	2	1±0	88	94	-6.8 %
12	Water Tanks	7	5	0.98±0.03	308	262	14.9 %
13	Fuel Oil	18	9	0.95±0.08	792	576	27.3 %
14	Marine Diesel Oil	3	3	1±0	132	144	-9.1 %
15	Gas Oil	4	3	0.96±0.08	176	148	15.9 %
16	Bilge and Sludges	2	2	1±0	88	94	-6.8 %
17	Others	3	2	1±0.01	132	97	26.5 %
18	LD Compressors	17	5	0.96±0.09	748	322	57.0 %
19	Fridges - Air Conditioning	4	4	1±0	176	196	-11.6 %
	Total	**182**			**8008**	**4523**	**43.5%**

Table 2. Obtained transmision results sending each vessel subsystem independently.

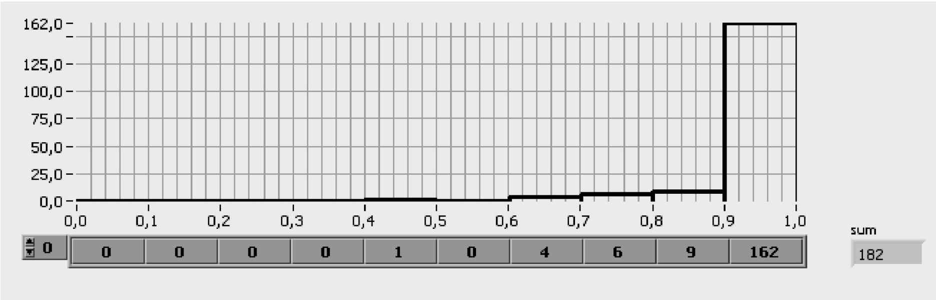

Figure 5. Histogram of coefficient of correlation *r* obtained sending each vessel subsystem independently. 162 (89 %) of them presented *r* between 0.9 and 1. All signal presented $r > 0.4$.

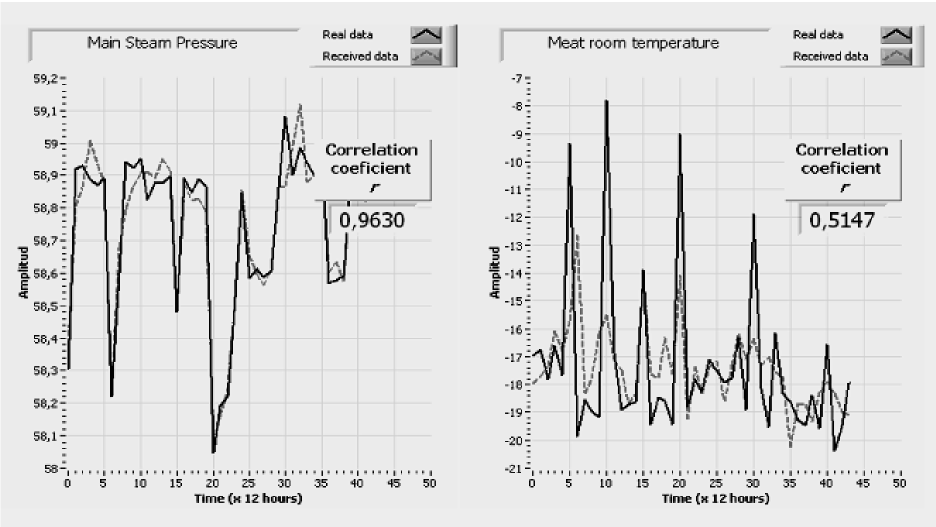

Figure 6. Two examples of onboard real signals (black line) and onshore received signal (red-dashed line) after PCA compression was applied. It is shown the case of sending all the 182 signals. The graph on the right represents the signal with the worst coefficient of correlation and in the left a signal with medium coefficient of correlation.

DISCUSSION

The best savings rates on the volume of transmitted data are obtained in power generation systems. These systems find strong correlations between different variables within it. The number of monitored signals of each subsystem is an important parameter, since those with less than 4 signals sampled data have the worst savings in the amount of data sent.

Between the two transmission strategies studied in this work, to send the full set of signals requires less data transmission rates (table 1: 46.9 % of saved money) than in separate subsystems (table 2: 43.5 % of saved money). However, this last strategy ensures that the dispersion of the correlation coefficients of the signals is less, improving fidelity in reception (figures 4 and 5).

It would be interesting to extend this study to other types of vessel, with other types of subsystems and operation forms.

CONCLUSION

The software developed for transmission using PCA significantly reduces the amount of data sent via satellite, reducing time and cost of communication in case of transmission of all signals together. Alternatively, PCA technique may increase the number of samples sent for a defined time and cost.

For some subsystems of the ship, the separate transmission of their signals is advantageous, bringing savings of 81.4% in the amount of data sent obtaining very high mean correlation coefficient ($r = 0.97 \pm 0.08$). For other subsystems, due to a low correlation between variables, the PCA is not advantageous with regard to sending the raw data. The software should detect these situations and use the most economical way.

PCA compression strategy is appropriate for making onshore maintenance decisions about onboard equipment with a strong correlation between sampled signals as propulsion subsystem, generation plant, etc, reducing communication cost.

ACKNOWLEDGMENTS

Our sincere thanks to the Castillo de Villalba ship crew and especially to D. Pablo Vegas, for his invaluable help.

REFERENCES

Belogolovy, A.; Belyaev, E.; Sergeev, A. & Turlikov, A. 2009: "Video Compression for Wireless Transmission: Reducing the Power Consumption of the WPAN Hi-Speed Systems", *Smart Spaces and Next Generation Wired/Wireless Networking, Proceedings*, vol. 5764, pp. 313-322.

Calvo, O.; Sousa, A.; Bibiloni, J.; Curti, G.; Acosta, G. & Rozenfeld, A. 2009: "Low-Cost Autonomous Underwater Vehicle for Underwater Acoustic Inspections", *Journal of Maritime Research*, vol. 6, no. 2, pp. 37-52.

Elbert, B.R. 1999: *The satellite communication applications handbook* Artech house, Norwood, Massachusetts.

Elbert, B. R. 2008: *Introduction to satellite communication*, 3rd ed edn, Artech House, Norwood, Massachusetts.

Gomariz, S.; Prat, J.; Gaya, P. & Sole, J. 2009: "An Autonomous Vehicle Development for Submarine Observation", *Journal of Maritime Research*, vol. 6, no. 2, pp. 23-36.

Grailu, H.; Lotfizad, M. & Sadoghi-Yazdi, H. 2009: "A lossy/lossless compression method for printed typeset bi-level text images based on improved pattern matching", *International Journal on Document Analysis and Recognition*, vol. 11, no. 4, pp. 159-182.

Horak, R. 2007: *Telecommunications and data communications handbook* Wiley-Interscience, Hoboken, New Jersey.

Johnson, K. J.; Rose-Pehrsson, S. L. & Morris, R. E. 2004: "Monitoring diesel fuel degradation by gas chromatography-mass Spectroscopy and chemometric analysis", *Energy & Fuels*, vol. 18, no. 3, pp. 844-850.

Khoo 2000: *Physiological control systems analysis, simulation, and estimation* IEEE Press etc., New York etc.

Lee, J. M.; Qin, S. J. & Lee, I. B. 2007: "Fault detection of non-linear processes using kernel independent component analysis", *Canadian Journal of Chemical Engineering*, vol. 85, no. 4, pp. 526-536.

Manly, B. F. J. 2005, *Multivariate statistical methods: a primer* Chapman and Hall, London etc.

Mason, R. L. & Young, J. C. 2002, *Multivariate Statistical Process Control with Industrial Applications* Society for Industrial and Applied Mathematics, Philadelphia.

Organización, M., I 1995: *G.M.D.S.S handbook handbook on the Global Maritime Distress and Safety System*, 2nd ed edn, International Maritime Organization, London.

Organización, M., I 2008: *Codigo NGV 2000 Código internacional de seguridad para naves de gran velocidad : resolucion MSC.97(73) adoptada el 5 diciembre de 2000, enmendada mediante las resoluciones MSC.175(79) y MSC.222(82)*, Edición de 2008, 2a ed edn, Organizacion Marítima Internacional, Londres.

Organización, M., I & Organización de Aviación Civil Internacional (Montreal, C. 2008): "Manual IAMSAR manual internacional de los servicios aeronáuticos y marítimos de búsqueda y salvamento", vol. Edición de 2008, 7a ed.

Peña Sánchez de Rivera, D. 1995: *Estadística modelos y métodos*, 2a ed. rev. edn, Alianza, Madrid.

Prasad, G. 2007: "On fusion of PCA and a physical model-based predictive control strategy for efficient load-cycling operation of a thermal power plant", *Optimal Control Applications & Methods*, vol. 28, no. 4, pp. 231-258.

Steinberg, Y. 2009: "Coding and Common Reconstruction", *Ieee Transactions on Information Theory*, vol. 55, no. 11, pp. 4995-5010.

Torokhti, A. & Friedland, S. 2009: "Towards theory of generic Principal Component Analysis", *Journal of Multivariate Analysis*, vol. 100, no. 4, pp. 661-669.

Xiong, L.; Liang, J. & Qian, J. X. 2007: "Multivariate statistical process monitoring of an industrial polypropylene catalyzer reactor with component analysis and kernel density estimatione", *Chinese Journal of Chemical Engineering*, vol. 15, no. 4, pp. 524-532.

Journal of Maritime Research, Vol. VII. No. 3, pp. 15-34, 2010
Copyright © 2010. SEECMAR

ISSN: 1697-4840

BIOFOULING GROWTH ON TUBULAR HEAT EXCHANGERS. MATHEMATICAL MODEL AND SIMULATION

A.Trueba[1,2]**, E. Eguía**[1,3] and **M.M. Milad**[1,4]

Received 23 February 2010; in revised form 20 May 2010; accepted 25 August 2010

ABSTRACT

Biofouling is one of the most serious problems to face numerous industrial processes. In the case of a tubular heat exchanger, biological deposits adhered to the inside surface of the tubes reduce heat transfer and therefore the thermal performance of the equipment. By virtue of this, control of this phenomenon is fundamental for both sea and land-based equipment to operate under optimal running conditions. A set of equations have been developed for this purpose which have enabled a mathematical model to be drawn up that is capable of predicting substrate and cell concentrations in the formation of biofilm over time, at any point in the tube. The said mathematical model serves as the basis for the creation of a computer simulation program that enables prediction of biofilm thicknesses and concentrations inside the tubes. It likewise allows experimentation with the heat exchanger under different working conditions and enables optimal down and cleaning times to be established.

Keywords: Biofouling, Heat exchanger, Mathematical model, Simulation.

INTRODUCTION

Biofouling may be defined as the undesirable phenomenon of adherence and accumulation of biotic deposits on an artificial surface that is submerged or in contact

[1] Department of Sciences & Techniques of Navigation and Ship Construction, Cantabria University, C/ Gamazo 1, 39004 Santander, Spain. [2]Assistant Professor Email: truebaal@unican.es [3] University Professor, Email: eguiae@unican.es [4] Ph.D. in Marine Sciences, Email: milad@ono.com.

with seawater. This accumulation consists of an organic film composed of micro-organisms embedded in a polymer matrix they themselves create (biofilm) that inorganic particles can reach and be retained (salts and/or corrosion products), which are the outcome of other types of fouling undergone in the process. This biofilm composed of micro-organisms (microbial biofouling or microfouling) may give rise to the accumulation of macro-organisms (macrobial biofouling or macrofouling) (Eguia et al., 2004).

The process whereby biofilm accumulates on a surface may be considered as the net result of several physical, chemical and biological processes (Characklis, 1990): The transport of soluble components and particles to the wet support medium, adsorption by the wet support medium, chemical or microbial reaction in the support medium or inside the deposit and separation, detachment or splitting of portions of the deposit layer.

The final outcome of this sequence of events is usually characterized by a sigmoid shaped progression or curve, in which three periods are clearly distinguishable (Eguía, 1998): In the first, known as induction, small changes are observed in the biofilm accumulation process; however, it is very difficult to appreciate any variation in representative parameters during this phase; the second, entitled exponential increase, is characterized by a logarithmic progression in the biofilm accumulation; and the third, called the asymptotic or flat phase, shows the stabilization of the biofilm accumulation process.

From the biofouling viewpoint, for a heat exchanger the following parameters should be considered:

— *Fluid parameters.* The type of fluid, its features and the conditions under which it fosters biofouling settlement are two of the most important factors to be taken into account in an industrial process. The factors relating to the fluid that should be taken into consideration for heat exchanger design are (Knudsen, 1991): Fluid purity and the absence of pollution; treatment of the fluid for the prevention of biological growth; treatment of the fluid to reduce biofouling; the influence of internal and external fluid flows and their velocity and temperature.

— *Heat exchanger parameters.* The exchanger parameters that exert a direct influence on biofouling settlement are: wall surface area and temperature, the material and coating used for the inside of the tube, geometry and protection systems.

— *Factors applied in heat exchanger design.* The consequences of the biofilm accumulation process on the tube walls are disastrous for heat exchanger performance; therefore in the design phase this phenomenon must be taken into account in the form of a fouling factor (Chenoweth, 1990).

A mathematical model is then constructed taking these variables into account, to predict substrate and cell concentrations over time, both in the liquid and biofilm phases, at any point in the heat exchanger tubes. The mathematical model enables a computer simulation program to be created in which it is possible to assess biofilm thicknesses and concentrations in the tubes under different working conditions. Thus, we can forecast the best down-times and cleaning times for keeping a seawater-cooled heat exchanger free of the biofouling phenomenon.

The growth simulation module for biofouling in heat exchangers is part of a computer design, simulation and analysis program that allows:

— The design and choice of the optimum tubular heat exchanger for a particular industrial process. The definition of the said heat exchanger is reached by following international standards, the recommendations of the classifying societies and current design methods used in modern industry today.
— The simulation of normal and abnormal operation in real, extreme working conditions to thus analyze and forecast to what point it can carry the process out without going into losses.
— The simulation of biofouling growth on exchanger walls and a forecast of the effects of the scale on exchanger performance.
— The forecast of the optimum operating time without losses in performance and the optimum down and cleaning periods.

MATHEMATICAL MODEL

The development of our mathematical model can be divided into four, well defined parts: the substrate concentration profile in the liquid phase; the substrate concentration profile in the solid phase; the cell concentration profile in the liquid phase; and the biofilm thickness.

The study was broached under the following assumptions (Characklis and Marshall, 1990): a.) The heat exchanger tubes are considered as a microbial tubular reactor; b.) Due to the high flow velocity in the tube, it was assumed that there is no cell reaction in the liquid phase; c.) In the biofilm formation process a liquid phase is clearly differentiated from a solid phase; d.) Matter in the liquid is transported by convection (transport of mass by fluid movement) and in by diffusion in the solid phase (transport of mass through a difference in concentration); e.) All the substrate considered in the liquid-biofilm interface is consumed by the organisms, therefore the wear by convection in the liquid phase is equal to the wear by diffusion in the solid phase; f.) Substrate transport and its concentration in the biofilm depends on the following variables: concentration in the liquid phase, flow velocity, resistance at the interface, substrate diffusion velocity in the biofilm, the velocity by which the organisms consume the substrate, cell mass concentration per unit of volume in the biofilm, the rate at which substrate is converted into cells and biofilm thickness; g.) Substrate diffusion velocity in the biofilm is very fast, therefore growth is at its maximum and the substrate reaction rate is the same in both the liquid and solid phases.

Mass Balance in the Liquid and Solid Phases (Biofilm)

By applying the Conservation of Mass Principle to the biofilm system, it is possible to determine the mass balances both in the liquid and solid phases where the substrate mass balance and the cell mass balance are taken into consideration for each of the phases. Thus, we can obtain the substrate and cell concentration at any point in the tube, in any phase and at any moment in time (Kotake and Hijikata, 1993). To obtain the substrate mass balance we apply the equation below

$$\frac{\partial S}{\partial t} + v\nabla S = D_s \nabla^2 S - r_s \quad (1)$$

and likewise for the cell mass balance

$$\frac{\partial X}{\partial t} + v\nabla X = D_x \nabla^2 X + r_x \quad (2)$$

The process states may be transitory when substrate and cell concentration at a particular point vary over time

$$\frac{dS}{dt} \neq 0, \ \frac{dX}{dt} \neq 0 \quad (3)$$

or stationary when the concentration does not vary over time

$$\frac{dS}{dt} = 0, \ \frac{dX}{dt} = 0 \quad (4)$$

Resolving equations (1) and (2) for each phase, substrate and cell concentration can be obtained at any point in the tube at any particular moment in time.

Substrate Concentration in the Liquid Phase

Taking equation (1) in a stationary state and given that in this phase, for a high flow velocity, transport by convection is much greater than by diffusion $(v\nabla S >> D_s \nabla^2 S)$

$$v\nabla S = -r_s \quad (5)$$

where

$$r_s = \frac{\mu_{máx}}{Y_s} X_f = q_{s_{máx}} X_f \quad (6)$$

therefore the substrate concentration at any point of the tube axis is

$$v\frac{dS}{dz} = -\frac{\mu_{máx}}{Y_s}X_f \tag{7}$$

By integrating equation (7) using the dimensionless variable method, where

$$S^* = \frac{S}{S_i}\ ,\ z^* = \frac{z}{L} \tag{8}$$

then

$$\frac{dS^*}{dz^*} = -\frac{\mu_{máx}}{Y_s}\frac{L}{vS_i}X_f = -k_m \tag{9}$$

therefore

$$\int_0^1 dS^* = \int_0^1 -k_m dz^* \tag{10}$$

We, thus, obtain the substrate concentration along the tube axis in the liquid phase and under stationary conditions, the process being represented by a straight-line graph with a gradient of $-K_m$.

The coefficient K_m represents the energy microorganisms require in their life process or the maintenance coefficient.

$$k_m = \frac{\frac{\mu_{máx}}{Y_s}X_f}{\frac{S_i}{L}v} = \frac{\text{consump}}{\text{transport}} \tag{11}$$

When $k_m = 1$, all the substrate entering the tube is consumed by the microorganisms.
When $k_m < 1$, there is sufficient substrate to fulfill the growth process.
When $k_m > 1$, the cell reaction is incomplete because there is insufficient substrate for all the organisms.

Substrate Concentration in the Solid Phase (Biofilm)

In the solid phase substrate is transported by diffusion (v = 0) and it is fully used up in the cell growth process, fulfilling Monod's saturation equation, which describes the relationship between microbial growth and substrate concentration

$$\mu = \frac{\mu_{máx} S}{k_s + S} \tag{12}$$

if $S = k_s$, then $\mu = \mu_{max}$, and growth does not depend on S.

if $S = k_s$ then $\mu = \frac{\mu_{máx}}{k_s}$, and growth is exponential and depends on S.

By applying equation (1) in a stationary state to the solid phase

$$D_s \frac{d^2 S}{dx^2} - r_s = 0 \tag{13}$$

assuming that $\mu = \mu_{max}$,

$$\frac{d^2 S}{dx^2} = \frac{\mu_{máx} X_f}{D_s Y_s} \tag{14}$$

And introducing the dimensionless variables

$$S^* = \frac{S}{S_b},\ x^* = \frac{x}{L_f} \tag{15}$$

then

$$\frac{d^2 S^*}{dx^{*2}} = \frac{2}{\Omega^2} \tag{16}$$

where Ω is the coefficient of substrate penetration in the biofilm, considering that if Ω >1, substrate penetration in the biofilm reaches the support medium and is complete and if Ω <1, penetration is incomplete; therefore in the layers furthest from the biofilm surface no microbial reaction takes place due to the lack of nutrients.

$$\Omega = \left[\frac{D_s S_b}{q_s X_f L_f^2} \right]^{1/2} \tag{17}$$

By integrating equation (17) for Ω >1 between $x^* = 0$ ($S^* = 1$) and $x^* = 1$ ($dS^*/dx^* = 0$)

$$S^* = \frac{x^{*2}}{\Omega^2} - \frac{2x}{\Omega} + 1 \tag{18}$$

and for $\Omega < 1$ between $x^* = 0$ ($S^* = 1$) and $x^* = x_A$ ($S^* = 0$)

$$S^* = \frac{x^{*2}}{x_A^{*2}} - \frac{2x^*}{x_A^*} + 1 \tag{19}$$

where

$$x_A^* = \frac{L_{fA}}{L_f} \tag{20}$$

Cell Concentration in the Liquid Phase

If a flocculation process takes place in the liquid phase, we will have an increase in the microbial population in the core of the liquid and thus a higher concentration of the said population. In the case of heat exchangers this process is not taken into consideration, due to the fluid velocity and the short time of residence available for completing the cell division; cell concentration is assumed only to vary due to adsorption, which consists of temporary or permanent immobilization of the cells contained in the fluid.

By applying equation (2) in a stationary state to the liquid phase, considering the flow speed in the tube axis to be z and making $r_x = r_{ax}$,

$$r_x = r_{ax} = k_{ax} X_L \left(1 - \frac{x_f'}{k_{ax}'}\right) \tag{21}$$

the cell mass balance in the liquid phase is

$$\frac{dX_L}{X_L} = \frac{k_{ax}}{v_z}\left(1 - \frac{x_f'}{k_{ax}'}\right) dz \tag{22}$$

Integrating for the condition $z=0$ ($X_L = X_{L0}$)

$$\ln X_L = -\frac{k_{ax}}{v_z}\left(1 - \frac{X_f}{X_{max}}\right) . z + \ln X_{L0} \tag{23}$$

and exponentially

$$X_L = X_{L0} EXP\left[-\frac{k_{ax}}{v_z}\left(1 - \frac{X_f}{X_{max}}\right) z\right] \tag{24}$$

where

$$z = z^{*} L \tag{25}$$

then for $0 < z^{*} < 1$

$$X_L = X_{L0} EXP\left[-\frac{k_{ax}}{v_z}\left(1 - \frac{X_f}{X_{max}}\right).z^{*} L \right] \tag{26}$$

Equation (26) enables us to calculate the cell concentration in the liquid phase along the tube axis of a heat exchanger while bearing only the adsorption process in mind and assuming that there is no growth in the liquid.

The cell adsorption process is calculated as the difference between cell mass at the inlet and outlet of the tube for $z^{*} = 0$ and $z^{*} = 1$

$$\Delta X_L = X_L\big|_{z^{*}=0} - X_L\big|_{z^{*}=1} \tag{27}$$

where this value is the cell concentration adhered to the internal surface of the tube that will go to form part of the biofilm formed on the support medium.

Cell Concentration in the Solid Phase. Biofilm Formation

Supposing that the cell mass per unit of biofilm volume remains constant over time, the accumulation of organisms and their growth contributes to increasing the biofilm thickness instead of increasing their concentration.

By applying equation (2) in a stationary state to the solid phase, the mass balance is

$$r_x = \frac{dX_f^{*}}{dt} = \frac{d}{dt}\left(\frac{A}{V} L_f X_f\right) \tag{28}$$

where

$$X_f^{*} = X_f \frac{A L_f}{V} \tag{29}$$

and the cell concentration at any moment in time is

$$X = \frac{X_0 e^{t\mu_{max}}}{1 - \frac{1}{X_{max}} X_0 (1 - e^{t\mu_{max}})} \tag{30}$$

In equation (28) if $\frac{A}{V} = \text{constant}$

$$r_x = \frac{A}{V}\left(L_f \frac{dX_f}{dt} + X_f \frac{dL_f}{dt}\right) \tag{31}$$

and if X_f is constant

$$r_x = \frac{A}{V} X_f \frac{dL_f}{dt} \tag{32}$$

given that

$$r_x = \mu X_f \tag{33}$$

then

$$\frac{dL_f}{dt} = \frac{\mu V}{A} \tag{34}$$

Resolving this differential equation for $t = 0$ and $L_f = L_{f0}$

$$L_f = \frac{\mu . V}{A} t + L_{f0} \tag{35}$$

this allows us to calculate the microbial growth process reflected in the increase in biofilm thickness at any moment without taking detachment due to fluid action into account.

SIMULATION OF THE BIOFOULING ACCUMULATION PROCESS IN A TUBULAR HEAT EXCHANGER

The formation of the biofilm on the submerged surface is an unavoidable consequence of a series of events that begin with the adsorption of organic molecules by the support medium surface, followed by bacterial adhesion, cell growth and reproduction and formation of extracellular polymers, finally constituting the biofilm matrix. For there to be a fast biofilm development, cell adhesion and reproduction levels must exceed those for detachment and death.

The development of a biofilm on a surface in contact with a fluid is the net outcome of various physical, chemical and biological processes, such as: transport of soluble components and particles from the fluid to the support medium; adsorption of cells on the support medium; chemical reactions on the support medium; production of exopolymers and other metabolic processes; and lastly the separation, detachment or splitting of portions of the deposit by the cutting force of the fluid or due to cell death.

If all these processes take place in series, the slowest stage of the sequence, called the determinant value stage or limiting value stage, may exert most influence and limit the value of the entire process. If the total process comprises a number of parallel processes and series-parallel processes, the slowest process then becomes the stage controlling value. It is necessary to identify the controlling value and the stage limiting value in order to correctly interpret the results of the experiment.

Description of the Simulation Module

The simulation and analysis process took place in a central tube of the heat exchanger, which was virtually fully insulated, and in which its dimensions and all its thermal-hydraulic flow parameters are maintained.

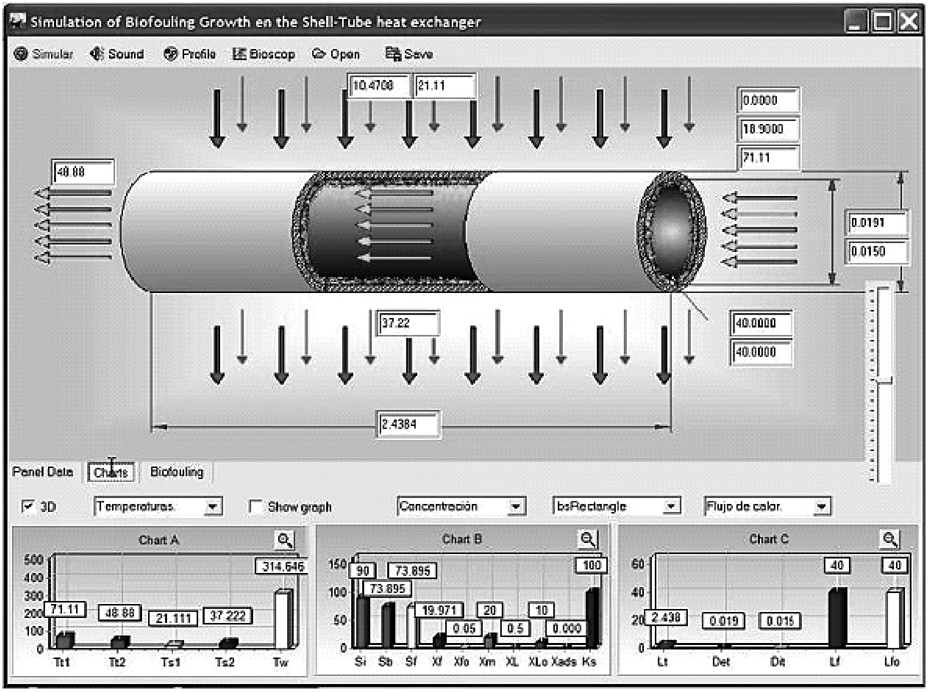

Figure 1. Main window of the simulation module

Figure 1 shows the main window of the simulation module, which offers the following alternatives:

— A virtual tube through which the heat transmission process takes place between fluids, and inside which a microbial growth and accumulation process occurs, giving rise to biofilm formation.

— The data cells on the drawing indicate the internal and external flow parameters and the dimensions of the tube.

— The data panel indicates the physical properties of the fluid from the tube (viscosity, density, specific heat and conductivity) and the flow's thermal-hydraulic parameters (heat transmission coefficients, heat transmitted, Reynolds Number and velocity).

— The graph panel provides a graph representation of how the biofouling accumulation parameters and the thermal-hydraulic flow parameters all evolve.

— The biofouling panel shows the simulation data and results referring to the accumulation, growth and elimination of the biofilm in the tube, such as substrate and cell concentration, growth rate, biofilm thickness and all the coefficients associated with microbial growth in a biofilm system. We only have to use the dropdown menus (see Figures 2a and 2b) to select the variable to be shown on the abscissa and ordinate axes to see a graph representation of their evolution.

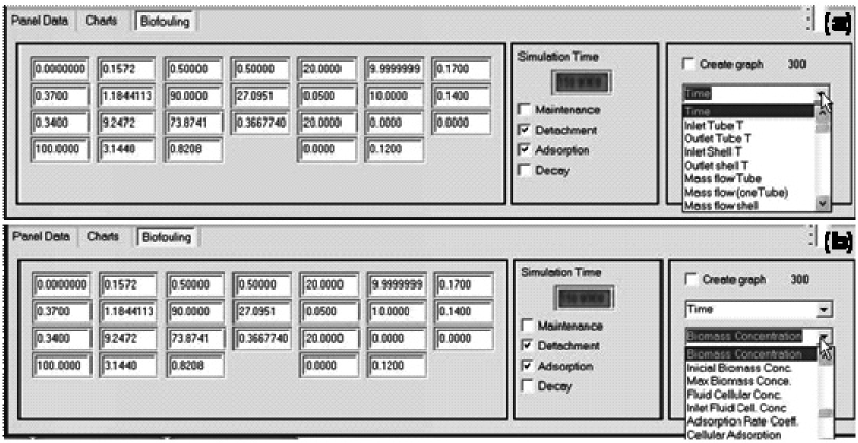

Figure 2. List of the parameters graphically represented on the abscissa axis (a) and the ordinate axis (b).

Simulation Process for Biofouling Accumulation

— Upload heat exchanger data. The program has a database which stores the characteristics of the heat exchangers designed which are going to be submitted to a simulation process for biofouling growth inside their tubes (see Figure 3).

— Biofilm Parameters. When a heat exchanger is simulated for the first time, it is necessary to put in the features of the fluid that circulates inside the tubes. The program automatically assumes the characteristics for the biofilm growth process.

— The "Bioscope" option enables us to forecast the variation in substrate and cell concentrations, as well as that of the biofilm over time. This is illustrated in Figure 4 for some specific initial conditions and a particular experiment period.

The program offers a wide range of possibilities. To be able to extract all the information it can provide and thus to understand the biofouling accumulation process and its effects on heat exchanger performance, we need at least a basic understanding of the processes of microbial transformation and growth in an aquatic medium, together with biofilm accumulation processes and mechanisms in heat exchangers and the effects of biofouling on their performance.

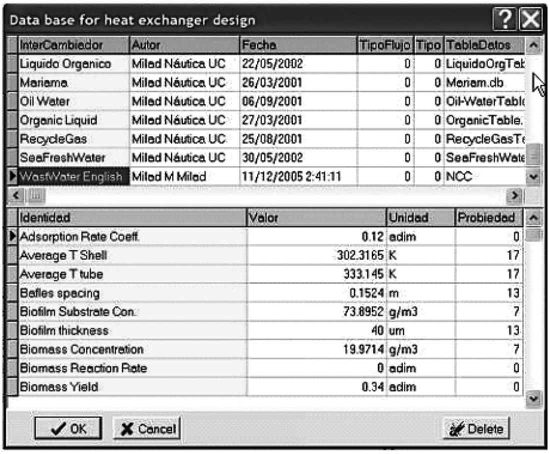
Data base for heat exchanger design

InterCambiador	Autor	Fecha	TipoFlujo	Tipo	TablaDatos
Liquido Organico	Milad Náutica UC	22/05/2002	0	0	LiquidoOrgTat
Mariama	Milad Náutica UC	26/03/2001	0	0	Meriam.db
Oil Water	Milad Náutica UC	06/09/2001	0	0	Oil-WaterTabl
Organic Liquid	Milad Náutica UC	27/03/2001	0	0	OrganicTable.
RecycleGas	Milad Náutica UC	25/08/2001	0	0	RecycleGasT
SeaFreshWater	Milad Náutica UC	30/05/2002	0	0	SeaFreshWate
WastWater English	Milad M Milad	11/12/2005 2:41:11	0	0	NCC

Identidad	Valor	Unidad	Probiedad
Adsorption Rate Coeff.	0.12	adim	0
Average T Shell	302.3165	K	17
Average T tube	333.145	K	17
Bafles spacing	0.1524	m	13
Biofilm Substrate Con.	73.8952	g/m3	7
Biofilm thickness	40	um	13
Biomass Concentration	19.9714	g/m3	7
Biomass Reaction Rate	0	adim	0
Biomass Yield	0.34	adim	0

OK Cancel Delete

Figure 3. Database of designed heat exchangers.

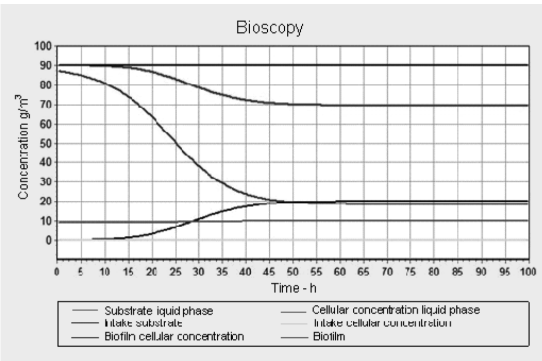

Figure 4. Evolution of substrate and cell concentration and the biofilm over time.

RESULTS

Figure 4 shows that the variation in substrate concentration in the liquid phase along the length of the tube for fifteen hours barely varies because the microbial population is very low and hence there is no consumption. From this point substrate consumption increased markedly at the same rate as the biofilm increases, to reach a stationary state after 60 hours where the substrate concentration no longer varies along the tube.

In the solid phase, substrate concentration varies from the liquid-biofilm interface to the tube wall because it is consumed by the organisms that comprise part of the biofilm. The curve gradient becomes steeper, which implies that there is a notable difference between the concentration on the biofilm surface and on the support medium. In some cases this may reach zero before reaching the support medium. This takes place when the biofilm is thick or cell metabolism is high and all the substrate arriving through the fluid is consumed. As time goes by, the substrate concentration in the biofilm tends to stabilize and reaches a stationary state, which depends on the cell concentration reaching its maximum saturation value.

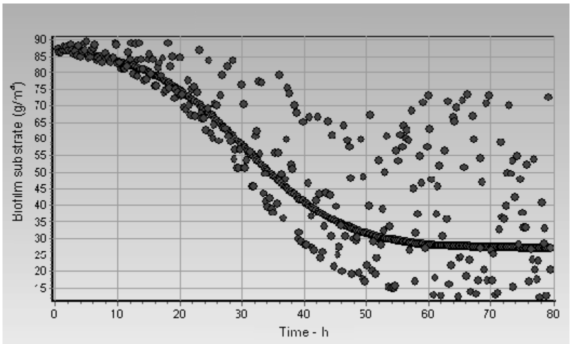

Figure 5. Evolution of substrate concentration at every point in the biofilm (●) and at its mid point (●●●●) from the surface to the support medium.

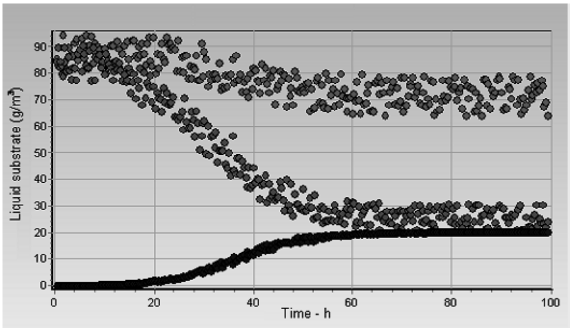

Figure 6. The effect of the variation in substrate concentration at the tube inlet on the concentration of substrate in the liquid (●), in the biofilm (●) and in the biofilm cell concentration (●●●●).

Figure 5 shows the simulation process of the evolution of biofilm substrate from the surface to the support medium, differentiating between substrate concentration at all the biofilm thickness points and the concentration in the middle of the biofilm.

Substrate concentration at the tube inlet has a direct effect on microbial activity and therefore on the organism population. To see the effect of the substrate concentration at the inlet, a variation is simulated from 80 to 95 g/m^3 for 100 operating hours. The results are shown in Figure 6, where we can see the effect of the said variation on substrate concentration at the tube inlet, on substrate concentrations in the liquid, in the biofilm and on concentration in the biofilm. We can see that cell concentration is only affected in the exponential growth phase, broadening the curve in the maximum growth phase to stabilize on reaching cell saturation concentration.

As far as the evolution of cell concentration is concerned, Figure 4 shows it develops through a slow linear phase followed by an exponential phase to the stationary state where concentration reaches its maximum. This state of maximum concentration depends on the organisms and on the nutrient concentration in the core of the liquid entering the tube. If the cell concentration is at its maximum, the increase in the microbial population increases the biofilm thickness and keeps the concentration constant. For small biofilm accumulations, the concentration increases exponentially whereas thickness increases with a smaller gradient. After a certain time saturation point is reached and cell concentration does not increase any further, however thickness does undergo an exponential increase.

The increase in the biofilm thickness depends on factors such as cell concentration, the specific growth rate, the concentration of organisms in the core of the liquid entering the tube and on substrate concentration. Biofilm thickness may rise slowly or exponentially depending on cell detachment or growth. These features may be simulated on the program producing the results shown in Figure 7. We can observe that when the detachment effect is unappreciable, biofilm thickness increases exponentially. On the other hand, whether there is a considerable detachment effect, it is especially detected early on in the process giving rise to a reduction in biofilm thickness until cell activity increases, thus leading biofilm thickness to rapidly increase. If the detachment effect is very large, either due to turbulences or to biofilm fragility, its thickness will stabilize and barely increase after some 60 hours.

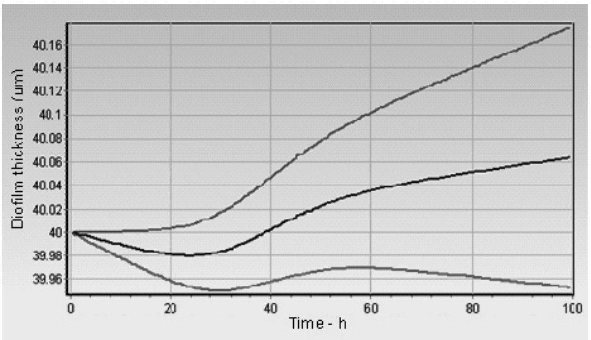

Figure 7. The comparative evolution of biofilm thickness over time: without detachment, with detachment, and with detachment in a stationary state

The effects of other parameters on biofilm thickness, such as specific growth rate, for example, can likewise be simulated to produce numerous graphs that provide a wealth of information.

CONCLUSIONS

This paper has applied an easily understandable mathematical model to one of the greatest problems facing seawater cooled industrial equipment –biofouling. This has enabled forecasts for substrate and cell concentrations to be made for the different phases of biofilm formation over time, at any point in the tube. Based on the mathematical model, the computer simulation program allows the thicknesses and concentrations of the biofilm in the tubes to be predicted and experiments to be carried out on the heat exchanger for different operating conditions. This, in turn, enables optimum down and cleaning times to be determined. The examples of the simulated effect caused by the variation in the biofilm formation process show the potential the simulation module offers. A variety of results and graphs can be obtained that enhance understanding of the biofouling accumulation process and its effects on heat exchanger performance.

NOMENCLATURE

A	biofilm surface
D	diffusion coefficient
K'_a	saturation coefficient per unit of volume
k_a	adherence coefficient
k_m	maintenance coefficient
k_s	saturation coefficient
L	tube length
L_f	biofilm thickness
q_s	specific consumption rate or consumption per mass cell unit and time unit in saturation state
r	reaction rate
r_a	specific adsorption rate
S	substrate concentration at a certain instance in time t
t	time
v	flow velocity
V	tube volume
X	cell concentration at a certain instance in time t
x	co-ordinate perpendicular to the tube axis
x'	cell concentration per unit volume
X_f	cell mass per unit of biofilm volume
Y	microbial mass produced per unit of substrate
z	co-ordinate in the direction of the tube axis

Greek-symbols

μ	specific growth rate
Ω	coefficient of substrate penetration in the biofilm

Subscripts

0	initial
A	biofilm thickness penetrated by the substrate
b	liquid-biofilm interface
f	solid phase
i	effluent
L	liquid phase
max	maximum
s	substrate
x	cell
z	direction of tube axis

Superscripts

*	dimensionless variable

REFERENCES

Characklis, W.G. (1990): Microbial Fouling. Biofilms, *Wiley Series in Ecological and Applied Microbiology*, 523-584.

Characklis, W.G. and Marshall, K. C. (1990): Biofilms: A Basis for an Interdisciplinary Approach. Biofilms. *Wiley Series in Ecological and Applied Microbiology*, 195-231.

Chenoweth, J. M. (1990): Final Report of the HTRI/TEMA Joint Committee to Review the Fouling Section of the TEMA Standards, *Heat Transfer Engineering*, 11 (1), 73-107.

Eguía, E. (1998): The Problem of Biofouling in Heat-Condensing Interchangers Cooled by Water of Sea. *Book Opening of the Academic Course 1998/1999*. Cantabria University. Spain, 29-41.

Eguía, E. and Trueba, A. (2004): Production of Environmentally Innocuous Coatings, *Journal of Maritime Research,* I (3), 5-22.

Hewitt, G.F. (1992): Handbook of heat exchanger design (HEDH). Begell House, Inc, New York, 1-33.

Knudsen, J.G. (1991): Conquer Cooling-Water Fouling, *Chemical Engineering Progress*, 87 (4), 42-48.

Kotake, S. and Hijikata, K. (1993): Numerical Simulations of Heat Transfer and Fluid Flow on a Personal Computer. *Transport Processes in Engineering, 3,* Elsevier, 1-368.

CRECIMIENTO DE BIOFOULING EN INTERCAMBIADORES DE CALOR TUBULARES. MODELO MATEMÁTICO Y SIMULACIÓN

RESUMEN

El *biofouling* es uno de los problemas más graves con que se enfrentan numerosos procesos industriales. En el caso de un intercambiador de calor tubular, los depósitos biológicos adheridos en la superficie interior de los tubos disminuyen la transferencia de calor y, por lo tanto, el rendimiento térmico del ciclo. Debido a esto, el control de este fenómeno resulta fundamental para que los equipos, tanto marítimos como terrestres, operen en condiciones óptimas de funcionamiento. Por ello se desarrolla un conjunto de ecuaciones que han permitido elaborar un modelo matemático con el que poder predecir las concentraciones de sustrato y celulares en las diferentes fases de formación de la biopelícula en el tiempo, en cualquier punto del tubo. Basándose en el modelo matemático elaborado se crea un programa de simulación informático que permite predecir espesores y concentraciones de biopelícula en los tubos pudiendo experimentar el intercambiador de calor en diferentes condiciones de funcionamiento y así conocer los tiempos de parada y limpieza óptimos.

MODELO MATEMÁTICO

En el desarrollo del modelo matemático se diferenciaron cuatro partes bien definidas: el perfil de la concentración del sustrato en la fase líquida, el perfil de la concentración de sustrato en la fase sólida, el perfil de la concentración celular en la fase líquida y el espesor de la biopelícula.

El estudio se abordó considerando los siguientes postulados (Characklis and Marshall, 1990): a.) los tubos del intercambiador de calor se consideraron como un reactor tubular microbiano, b.) debido a la alta velocidad del flujo en el tubo se supuso que no hubo reacción celular en la fase líquida, c.) en el proceso de formación de la biopelícula en los tubos se diferenció entre una fase líquida y una fase sólida, d.) la materia en el líquido se transporta por convección (transporte de masas por movimiento del fluido) y en la fase sólida por difusión (transporte de masas por diferencia de concentraciones), e.) todo el sustrato considerado en la interfase *líquido-biopelícula* es consumido por los organismos, por lo que el gasto por convección en la fase líquida es igual al gasto por difusión en la fase sólida, f.) el transporte del sustrato y la concentración en la biopelícula depende de las siguientes variables: concentración en la fase líquida, velocidad del flujo, resistencia en la interfase, velocidad de difusión del sustrato en la biopelícula, velocidad de consumo del sustrato por los organismos, concentración de masa celular por unidad de volumen en la biopelícula, tasa de conversión de sustrato en células, espesor de la biopelícula, g.) la velocidad de difusión del sustrato en la biopelícula es muy rápida, por lo que el crecimiento es máximo, siendo la tasa de reacción del sustrato la misma en la fase líquida que en la sólida.

SIMULACIÓN DEL PROCESO DE ACUMULACIÓN DE BIOFOULING EN UN INTERCAMBIADOR DE CALOR TUBULAR

Descripción del módulo de simulación

El proceso de simulación y análisis se realizó en un tubo central del intercambiador de calor, virtualmente aislado, en el que se mantienen sus dimensiones y todos los parámetros del flujo termohidráulico. En la Figura 1 se presenta la ventana principal del módulo de simulación, la cual ofrece las siguientes posibilidades:

— Tubo virtual a través del cual se produce el proceso de transmisión de calor entre fluidos, en cuyo interior se experimenta el proceso de crecimiento y acumulación microbiana que origina la formación de biopelícula.
— Las celdas dispuestas en el dibujo indican los parámetros del flujo interno y externo y las dimensiones del tubo en cuestión.
— El panel de datos indica las propiedades físicas del fluido del tubo (viscosidad, densidad, calor específico y conductividad) y los parámetros termohidráulicos del flujo (coeficientes de transmisión de calor, calor transmitido, número de Reynolds y la velocidad).
— El panel de gráficos presenta de manera gráfica la evolución de los parámetros del proceso de acumulación del biofouling y de los parámetros del flujo termohidráulico.
— El panel biofouling presenta los datos y resultados de la simulación referentes al proceso de acumulación, crecimiento y eliminación de la biopelícula en el tubo, tales como, la concentración del sustrato y celular, tasa de crecimiento, espesor de la biopelícula y todos los coeficientes asociados al crecimiento microbiano en un sistema biopelícula. Basta con seleccionar en los "desplegables" (ver Figura 2a y 2b) la variable a representar en los ejes de abscisas y ordenadas para ver gráficamente su evolución.

Proceso de simulación de acumulación de biofouling

— Carga de los datos del intercambiador de calor. El programa dispone de una base de datos en la que se almacenan las características de los intercambiadores de calor diseñados, a los que se va a someter al proceso de simulación de crecimiento de biofouling en el interior de sus tubos (ver Figura 3).
— Parámetros de la biopelícula. Cuando se simula un intercambiador de calor por primera vez es necesario introducir las características del fluido que circula por el interior de los tubos. Las características propias del proceso de

crecimiento de la biopelícula las asume el propio programa de manera automática.

— La opción "Bioscopio" permite predecir la variación de la concentración de sustrato y celular, así como de la biopelícula en el tiempo, tal y como se muestra en la Figura 4 para unas condiciones iniciales dadas y un periodo de experimentación determinado.

Las posibilidades del programa son amplias y para poder extraer toda la información que puede aportar y así comprender el proceso de acumulación de biofouling y sus efectos en el rendimiento del intercambiador de calor hay que tener un mínimo conocimiento sobre el proceso de transformación y crecimiento microbiano en el medio acuático, así como de los procesos y mecanismos de acumulación de la biopelícula en los intercambiadores de calor y de los efectos del biofouling en su rendimiento.

CONCLUSIONES

Este trabajo ha aplicado un modelo matemático fácil de comprender a uno de los mayores problemas con que se enfrentan los equipos industriales refrigerados con agua de mar: el biofouling. Esto ha permitido predecir las concentraciones de sustrato y celulares en las diferentes fases de formación de la biopelícula en el tiempo, en cualquier punto del tubo. Basándose en el modelo matemático el programa de simulación informático permite predecir espesores y concentraciones de biopelícula en los tubos pudiendo experimentar el intercambiador de calor en diferentes condiciones de funcionamiento y así conocer los tiempos de parada y limpieza óptimos. Los ejemplos de simulación del efecto de la variación de algunos parámetros en el proceso de formación de la biopelícula, muestran las posibilidades del módulo de simulación. Pueden obtenerse una variedad de resultados y gráficos que ayudan a la compresión del proceso de acumulación del biofouling y sus efectos en el rendimiento del intercambiador de calor.

Journal of Maritime Research, Vol. VII. No. 3, pp. 35-42, 2010
Copyright © 2010. SEECMAR

Printed in Santander (Spain). All rights reserved
ISSN: 1697-4840

THE INFLUENCE OF THE STATIC PARTS MASS OF A MACHINE ON ITS NATURAL FREQUENCIES OF VIBRATION

A. De Miguel[1,2], **A.M. Costa**[1,3] and **F. Antelo**[1,4]

Received 14 April 2010; in revised form 27 May 2010; accepted 14 September 2010

Abstract

In this article it is intended to highlight the importance of choosing correctly the stationary parts mass in a machine to reduce the amplitude of the vibrations produced by moving parts of it, and in order to control its natural frequencies of vibration to try to avoid critical speeds during its normal performance. We have made three simulations, in which we have kept constant all parameters that influence in the natural frequency of the machine and we have changed one, the mass of the static parts of it.

Keywords: Machine, vibration, natural frequency, amplitude, unbalanced, damping.

INTRODUCTION AND ASSUMPTIONS

The problems generated by the engines and machines vibrations are several, but all of them have a common factor the machine lifetime reduction. For this reason it is so important understand how the problem is generated to try to find a more suitable solution for this particular problem.

Assuming that any machine is made with reciprocating and rotating moving elements and other static; the rotating parts balancing is not perfect, so they can be both statically and dynamically unbalanced (in the first the centre of gravity of the piece is

[1]Department Enerxía e Propulsión Mariña, Universidade da Coruña, maradc00@udc.es, Tel. 622297294, c/paseo de ronda n 51, 15011 A Coruña, Spain. [2] Doctoral student, Email: maradc00@udc.es, [3] Doctoral student, Email: am_lito@hotmail.com. [4]Associate professor, Email: fantelog@udc.es.

outside the rotation axis, which generates a inertial force uncompensated; in the second the change of the angular momentum is not zero, producing a inertial torque uncompensated). The movement of parts with reciprocating motion also generates alternative inertial forces that induce the vibration of the whole machine.

This vibration is generated in a continuous medium, in this mass, friction and stiffness of the system are located along all parts, therefore the system has infinite degrees of freedom and infinite natural frequencies, which causes that mathematical analysis would be very complex. In order to resolve this mathematical problem; the best way to get a very approximate solution to the exact solution is to use iteration methods such as:

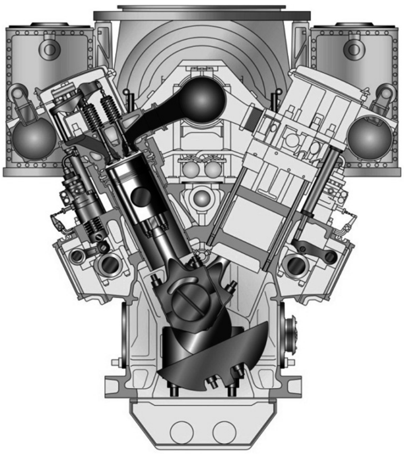

Figure 1. View of a generic machine.

Stodola method: it is an iterative process used to calculate of the main modes and natural frequencies of no-damped vibration systems. It is a physical mean and it does not need to derive the differential equation of the motion.

Matrix iteration: it is another iterative process that lead to the main modes of a vibration system and its natural frequencies, the displacements of the masses to be approximately, and base on these shifts it is obtained the system matrix equation, which is developed and finding the first vibration mode, and others are obtained by orthogonality principle.

Holzer method: it is a tabular method valid for any system, in which it is made the successive assumptions of the natural frequencies of the system which is based on the calculation of the frequencies calculated in the previous steps.

Another option is to simplify the system to one equivalent with fewer freedom degrees, which is easier to analyze, and of this way we can obtain similar results for both analyses being the last simpler than first.

MATERIAL, METHODS AND EQUATIONS

To simplify the system it is going to reduce all the parts that constituting the machine by a single mass and equivalent to all parts of the same, to calculate this mass it is used the notion of reduced mass. The distributed mass system with a rather complex motion (rotation, alternative or combined) is replaced by a mass concentrated at a point and a translational motion, this mass is called the reduced mass of the system in question, and this reduced mass is equivalent to the original with respect to kinetic energy "*T*".

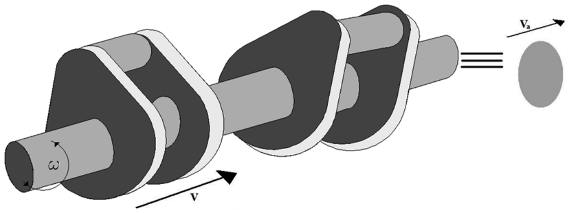

Figure 2. Identification of a system with a particle with mass.

To determine the value of this mass is necessary to identify the total kinetic energy of the machine to the mass of the particle *"A"*, for a machine this procedure is relatively simple since all machine parts have moving plane, a fact which greatly simplifies equation:

$$\boldsymbol{T_{mach}} = \sum_{\boldsymbol{i=0}}^{\boldsymbol{n}} {}^{1}/_{2}\, I_i \omega_i{}^2 + \sum_{\boldsymbol{i=0}}^{\boldsymbol{n}} {}^{1}/_{2}\, m_i v_i{}^2 \;\equiv\; {}^{1}/_{2}\, M v_a{}^2\,; \tag{1}$$

The kinetic energy of the machine "T_{mach}" is equal to the second term of the equation (1) and we identify this with the kinetic energy of a particle of mass "m_a" and velocity "v_a". To increase the simplifications in the calculation of "m_a" we assume that "v_a" is equal to 1 m/s, so the equation is simplified to the maximum.

The procedure to determine the system equivalent stiffness and damping coefficient it is similar to finding the reduced mass, to calculate the stiffness coefficient is used elastic energy of deformation of all parts of the machine with a elastic energy of a spring whose coefficient of stiffness will be *"K"*, for the equivalent damping coefficient is identifying all the energy dissipated by the system (internal friction, friction with the lubricant and bearings ...) with the energy dissipated by a damper whose constant was *"C"* is moving at a velocity "v_a".

DEVELOPMENT PHYSICAL-MATHEMATICAL

With these considerations is done to simplify the equation of motion of the continuous system by the equation of the equivalent system, with only one degree of freedom, which is assumed to exist displacement in only one direction (displacement in the other directions and rotations are obvious, without loss of generality) to further simplify the analysis; to obtain the equation using the principle of D'Alembert and assuming that the motion of the mass is simple harmonic and therefore its position has the form , in the light of free-body diagram we can see:

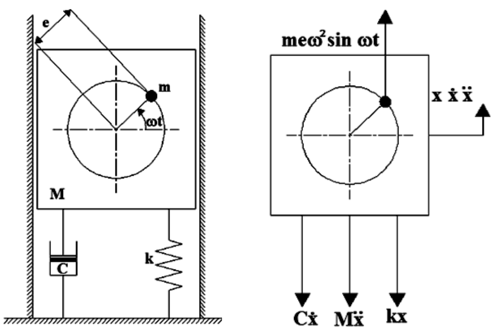

Figure 3. Problem to be studied and vector diagram of forces.

$$M\ddot{x} + c\dot{x} + kx = me\omega^2 \,\text{sen}\, \omega t \tag{2}$$

The meaning of each term is the next:

— $M\ddot{x}$: Is the inertial force that acting on the set of the machine.

— $M\dot{x}$: Is the damping force, by which the energy of the system is dissipated like heat.

— *kx*: Is the elastic deformation force.

— $ne\omega^2 \sin \omega t$: It represents the force generated by the vibration of the system, "m" is the unbalanced mass and "e" is the distance from the axis of rotation to "m", y "ω" is the frequency of the machine, this force can be centrifugal force or a first order force actuating on the reciprocating piston.

By theory of vibrations the solution to this equation for one variable "x" is an expression like:

$$x = \left[Ce^{-\zeta\omega nt}\,\text{sen}(\omega dt + \phi)\right] + \left[\frac{me\omega^2}{\sqrt[2]{(k - M\omega^2)^2 + (C\omega)^2}}\,\text{sen}(\omega t - \psi)\right] \tag{3}$$

The first term of the right side of the equation (3) represents the response of the transient statement , which has no relative importance because it disappears with over time; the second term of that represents the steady state response of the system and whose analysis is really important to study to know the parameters of the vibration of the machine such as amplitude, frequency... Otherwise writing the second term in the expression above:

$$x = \frac{\frac{me\omega^2}{k}}{\sqrt[2]{\left[1-\left(\frac{\omega}{\omega_n}\right)^2\right]^2 + \left[2\zeta\left(\frac{\omega}{\omega_n}\right)\right]^2}}\,\text{sen}(\omega t - \psi) \tag{4}$$

Where each term ha the usual meaning as defined in the theory of vibrations, but we will explain the most important "ω_n" the natural frequency of the system for this case is calculated as $\sqrt[2]{\boldsymbol{k/M}}$ is a fundamental parameter because it defines the resonance condition of the system, in this situation the amplitude of the vibration is only limited by damping factor "ζ" of the system, as this value is reduced vibration amplitude tends to infinity, hence the importance of choosing appropriate the values of: "*k*", "*M*" and "c" so the natural frequency of the system are far from the frequencies that excite the system "ω" (for a continuous medium that possesses infinite natural frequencies this conclusion, that the natural frequency must be far from the excitation frequencies, is the same).

From the above equation it also follow that if increased “M” (mass of the whole machine) for “m” (unbalanced mass that induces the vibration) the amplitude of vibration is reduced by reducing it also reduces the deformation of the pieces, what causes mechanical stress that occurs because of the vibration also decreases, since both are proportional (assuming that the parts are working as perfectly elastic, that is common practice).

DEVELOPMENT OF SIMULATED PROBLEM

The following figure represents a simulation of the proposed problem, to show that everything which follows from the theory of vibrations is met. This scheme is generated to simulate this problem is as follows:

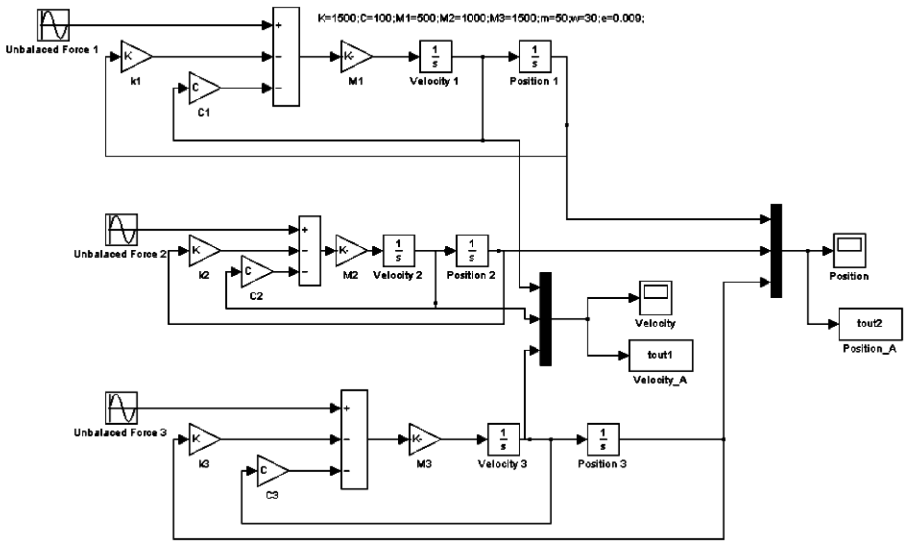

Figure 4. Scheme of equation that is evaluated.

In the previous scheme that is seen is the simulation of the next equation:

$$M\ddot{x} + c\dot{x} + kx = me\omega^2 \operatorname{sen} \omega t \quad (5)$$

In this scheme, what is done is to select functional blocks of a specific program of simulation, where each one performs a mathematical operations (sum, multiplication, logarithms, integrals…) represents a constant, a variable of the problem… what you do with these blocks is to fill them properly and unite them to build the desired equation.

But in this case we have done three simulations where are varying in each mass *"M"* which represents the mass of the static parts of the machine under study, in the first case is given the value of 500 kg. in the second of 1000 kg. and in the third 1500 kg. The other parameters are the same for all cases, friction constant *"c"*, stiffness constant *"k"*, the unbalanced mass *"m"* that generated the vibration…

RESULTS

The results of three simulations are the next figures:

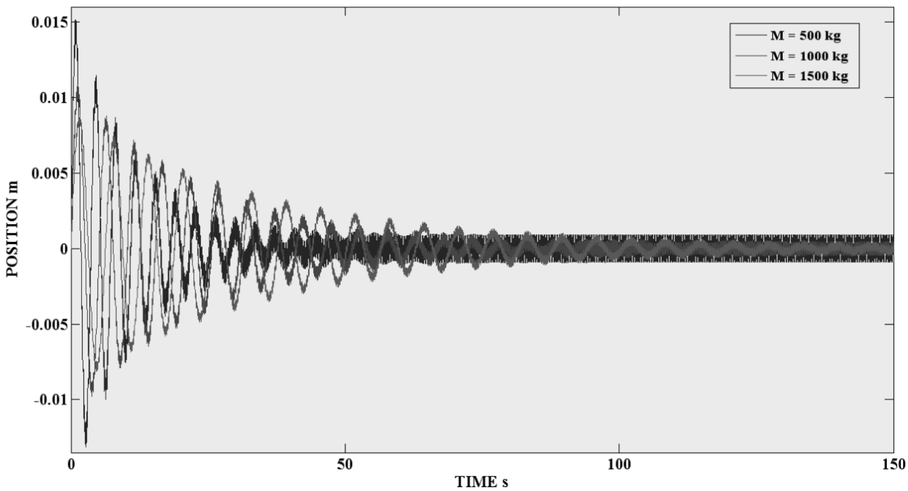

Figure 5. Results of a simulation, position versus time.

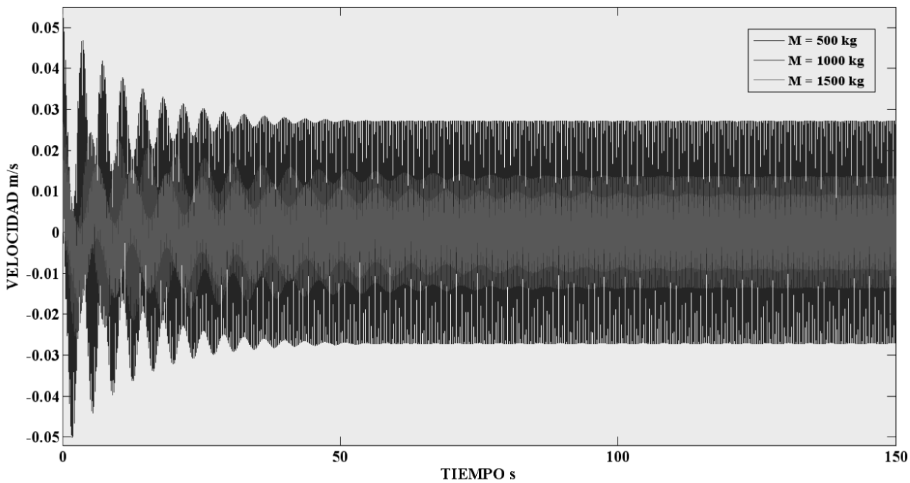

Figure 6. Results of a simulation, velocity versus time.

The figures 5 and 6 show the position and the velocity of vibration for one of each example simulated above. In this figures we can see the transient state and the steady state; in addition we can see how change the results when is changed the mass of static parts of the machine *"M"*.

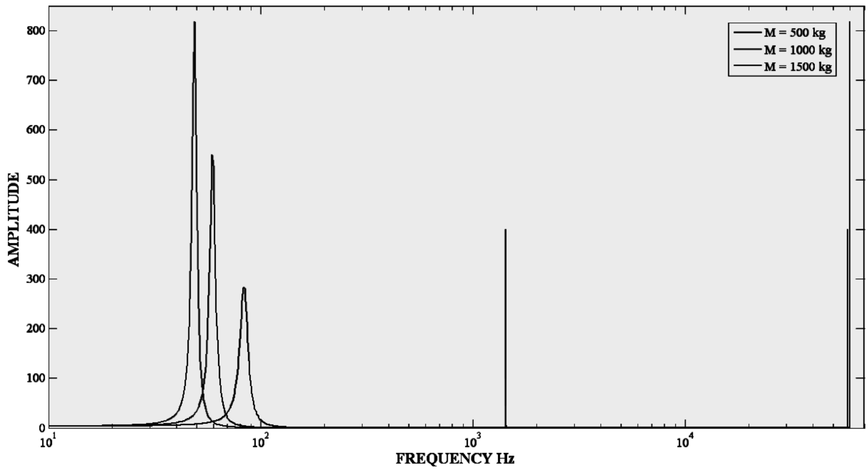

Figure 7. Results of a simulation, Spectrum of the systems.

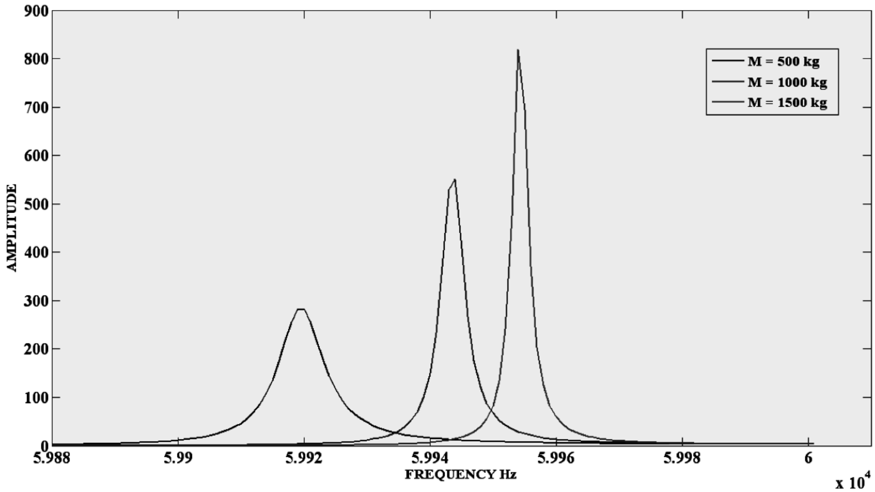

Figure 8. Results of a simulation, detail of a spectrum of the systems.

The figures 7 and 8 show the spectrum of vibration for one of each example simulated above. In this figures we can see the frequencies of the vibration; the frequencies between 30 and 100 Hz and over 60.000 Hz are the natural frequencies of vibration of each example and the frequencies over 1.400 Hz is the frequency of the excitation of unbalanced mass *"m"*.

From the above figures we can obtain a set of conclusion that would be difficult to obtain if we would have analyzed the equation mathematically and the response for each of the examples that we have assumed.

CONCLUSIONS

- — The amplitude and the velocity (also the acceleration, as is not represented) of the vibration decrease when the mass of the machine *"M"* increase.
- — The frequency of vibration on transient state is different for each instance, because of the variation of natural frequency "ω_n" by varying the total mass of the machine and not its stiffness.
- — At steady state the only difference observed is the amplitude and the velocity of the vibration, but the frequency is the same for the three instances.
- — By increasing the static mass increases the amplitude in the harmonics but decreases in the fundamental frequencies; and also the opposite happens; so the designer can modify the parameters of the vibration.
- — The mass of the static parts does not have influence in the frequency during steady state, but it is fundamental on transitional arrangements.

REFERENCES

Pérez, C. (2002): *Matlab y sus aplicacións en las ciencias y la ingeniería.* Pearson Prentice Hall.

Seto, W. (1970): *Vibraciones mecánicas*. McGraw-hill.

Timoshenko, S. (1970): *Vibration problems in engineering.* D. Van Nostran company, INC.

Haider N. A., Nayfeh A. H. and Faris W. (2003): Natural frequencies of heated annular and circular plates. *International Journal of Solids and Structures,* Vol. 41 pp. 3031-3051. 2004 Elsevier Science Ltd. Available from: www.elsevier.com/locate/ijsolstr.

Akulenko L.D. (1998): High-frequency tural oscilations of mechanical systems. *Journal of Applied Mathematics and Mechanics,* Vol.64, No. 5, pp. 783-796. 2001 Elsevier Science Ltd. Available from: www.elsevier.com/locatc/jappmathmech.

Bartelmus W. and Zimroz R. (2007): Vibration condition monitoring of planetary gearbox under varying external load. *Mechanical Systems and Signal Processing,* Vol.23 pp. 246–257 2009 Elsevier Science Ltd. Available from: www.elsevier.com/locate/jnlabr/ymssp.

http://www.fysik.uu.se/kurser/fy660/compendium/Signal/FFTmatlab.htm

Journal of Maritime Research, Vol. VII. No. 3, pp. 43-56, 2010

ISSN: 1697-4840

SEA PIRACY AND MARITIME SECURITY: THE PROBLEM OF FOREIGN NAVAL INTERVENTION IN THE SUPPRESSION OF PIRACY OFF THE HORN OF AFRICA

F.C. Onuoha[1] and **G.E. Ezirim**[2]

Received 18 May 2010; in revised form 6 June 2010; accepted 29 September 2009

Abstract

Waters off the Horn of Africa (HoA) are strategic for global commerce and international security. Since 2005 this vital waterway has remained the world's most dangerous hotspot of piracy, prompting states whose economic and security interests are particularly being undermined by spiralling piracy in the region has deployed their navies to help enhance maritime security. This article conceptualizes the relationship between sea piracy and maritime security in relation to foreign naval intervention, highlights the continuance and trend of pirate incidence off the HoA, discusses the emerging risks associated with the intervention of foreign navies in the fight against piracy, and proffers some measures that could contributed to suppressing piracy in the region. It contends that achieving sustainable maritime security in Africa demands that the root causes of piracy in Africa is effectively tackled, rather than reacting to the symptom of a deeper malaise.

Keywords: Security, Sea Piracy, Maritime Security.

INTRODUCTION

Waters off the Horn of Africa (HoA) are strategic for global commerce and international security. However, since 2005 this vital waterway has remained the world's most dangerous hotspot of piracy. Growing piracy in the region has elicited the

[1]Research Fellow, National Defence College Nigeria, Email: chufreedom@yahoo.com, Tel. +2348037791916, Herbert Macaulay Way North, 00009 Abuja, Nigeria. [2]Lecturer, SGSS University of Nigeria Nsukka, Email: ekenezirim@yahoo.com, Tel. +2348037844707, University of Nigeria Nsukka, 00004 Nsukka, Nigeria.

attention of the United Nations, States, security analysts and scholars. Given its importance for international merchant shipping, states whose economic and security interests are particularly being undermined by spiralling piracy in the region has deployed their navies to help enhance maritime security. Warships from over 20 countries now patrol the waters off the HoA in an effort to protect shipping routes. The intervention of international naval task force shows just how serious the problem of piracy has become in the region. In spite of the presence of a flotilla of foreign naval warships, the incidence of piracy has continued and is spreading to new areas.

This article conceptualizes the relationship between sea piracy and maritime security in relation to foreign naval intervention, highlights the continuance and trend of pirate incidence off the HoA, discusses the emerging risks associated with the intervention of foreign navies in the fight against piracy, and proffers some measures that could contribute to suppressing piracy in the region.

CONCEPTUAL FRAMEWORK

The framework of analysis adopted here interprets the nexus between sea piracy and maritime security as interfacial (Onuoha, 2009). It begins with a conceptual clarification of terminologies and proceeds to offer a schematic illustration of the perceived relationships.

The term 'sea piracy' has been defined in different ways by scholars, states, and organisations. Essentially, piracy is a term used to describe acts of armed robbery, hijacking and other malicious acts against ships in international waters. They are carried out with the intent of stealing valuables onboard and/or extorting money from ship owners and/or other third party interests by holding the ship or crew to ransom (OCIMF, 2009). The United Nations Convention on the Law of the Sea (UNCLOS) defines piracy as consisting of any of the following acts:

(a) any illegal acts of violence or detention, or any act of depredation, committed for private ends by the crew or the passengers of a private ship or a private aircraft, and directed:
   (i) on the high seas, against another ship or aircraft, or against persons or property on board such ship or aircraft;
   (ii) against a ship, aircraft, persons or property in a place outside the juris diction of any State;
(b) any act of voluntary participation in the operation of a ship or of an aircraft with knowledge of facts making it a pirate ship or aircraft;
(c) any act inciting or of intentionally facilitating an act described in sub-paragraph (a) or (b) (UNCLOS, 1982).

Therefore, for such a crime to qualify as piracy, which is an international crime, the illegal act or crime must be carried out on the high sea, which is outside the twelve mile limit of the territorial waters of a maritime state (Vogt, 1983). It is evident from the above definition that acts of violence against ships, especially those that occur in ports or territorial waters are not regarded as "piracy" under international law. They are therefore classified as "armed robbery"[1]. However, an estimated 80 per cent of so-called 'piracy' is not piracy on the high sea as legally defined, but raiding in territorial waters (Pugh and Gregory, 1994).

Given that most attacks against ships take place within the jurisdictions of States and piracy as defined under UNCLOS (1982) does not address this aspect, this paper adopts the definition of piracy offered by the IMB as 'the act of boarding any vessel with the intent to commit theft or other crime and with the capability to use force for furtherance of the act' (IMB, 1997). Although this definition does have some loopholes, it serves the useful purpose of providing a context for finding evidence and statistics on reported attempts or actual boarding of a vessel by an individual or group with the intent of stealing the vessel's contents or for achieving other personal benefits.

Maritime security in this context refers to the freedom from or absence of those acts which could negatively impact on the natural integrity and resilience of any navigable waterway or undermine the safety of persons, infrastructure, cargo, vessels and other conveyances legitimately existing in, conducting lawful transactions on, or transiting through territorial and international waterways. Geographically, the maritime domain of a coastal state includes territorial waters, measured as 12 nautical miles from the coast; the contiguous zone or coastal waters, calculated as 24 nautical miles from the coast; the exclusive economic zone, which is 200 nautical miles from the coast; and last, the continental shelf, which can extend out to 350 nautical miles from the coast (Rooyen, 2009).

Maritime security has two principal dimensions. The first is the intrinsic dimension, which is concerned with the natural integrity of all elements that form the basic and essential features of the maritime domain, such as the pristine quality of the waters and the quantity of fish and other marine resources. The second dimension, the extrinsic dimension of maritime security, covers the safety of all 'foreign' objects, which do not form part of the basic and essential features of the marine ecosystem but exist or make use of the maritime domain.

Thus, both international and territorial waterways provide the environment for piracy. Indeed, the potential for sea piracy exists along almost all waterways, whether of advanced or developing countries. However, the degree of its manifestation in a particular location is usually a function of the nature of measures adopted to achieve maritime security. Therefore, the state of maritime security and piracy are interfacial

[1] For critical remarks on the drafting deficiencies of the UNCLOS's (1958; 1982) definition of piracy, and how this undermines international efforts aimed at combating maritime piracy, see H.E.J. Luis Jesus, "Protection of foreign ships against piracy and terrorism at sea: Legal Aspects", *The International Journal of Marine and Coastal Law*, 18, 3, (2003), esp. pp. 375-380; Samuel P Menefee, "Foreign Naval Intervention in Cases of Piracy: Problems and Strategies", *The International Journal of Marine and Coastal Law,* 14, 3, (1999), esp. pp. 358-361.

and integrally related. This is what is indicated by the thick straight line (a) dividing the two variables into two equal parts in Figure 1. Thus, when piracy increases (+), it reduces maritime security (-). Conversely, increase in the level of maritime security (+) usually translates to decrease in the level of sea piracy (-), as indicated by the movement of the broken line (b).

Figure 1. Sea Piracy and Maritime Security Linkage.

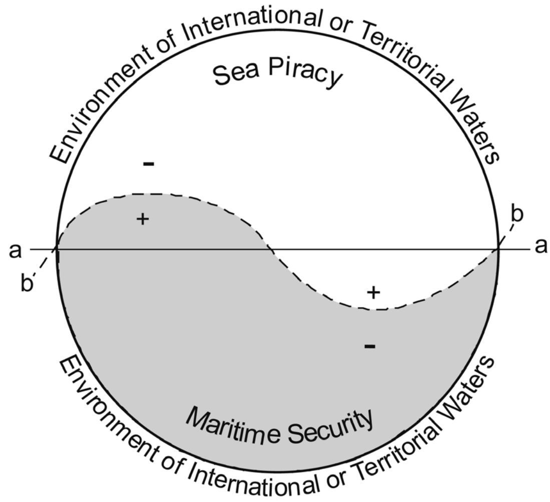

Source: Freedom C. Onuoha, "Sea Piracy and Maritime Security in the Horn of Africa'

In this sense, sea piracy threatens the two observed dimensions of maritime security. In terms of the intrinsic dimension, an environmental disaster resulting from pirate violence against oil-laden ships would undermine the marine ecosystem and in turn threaten a country's food supply and local livelihoods. With regard to the extrinsic dimension, piracy poses common risks to those who use the maritime environment, irrespective of their nationality or activity – among other vessels and their crews, tourists, workers on oil rigs. Therefore the task facing coastal states is to design and implement robust and sustainable (legal, political, economic, transnational and military) measures that would buoy up maritime security and reduce sea piracy.

The extrinsic dimension of maritime security has gained renewed emphasis in recent times, partly for two reasons. The first and perhaps the remote factor is the growth in transnational organised crimes that make use of the high seas – narco-trade, oil bunkering, piracy, small arms and light weapons smuggling – especially in but not limited to Africa, including the tendency to finance terrorism through these illicit trades. The second and a more proximate factor is the growing threat of international terrorism, especially since the 9/11 attacks in 2001. This has necessitated the adoption of some measures to enhance maritime security, including the introduction of the International Shipping and Port Security (ISPS) Code, Proliferation Security Initiative (PSI), Container Security Initiative, and the Customs-Trade Partnership against Terrorism, to protect merchant shipping.

Therefore the task facing coastal states is to design and implement robust and sustainable (legal, political, economic, transnational and military) measures that would enhance maritime security by suppressing maritime threats. Hence, the intervention of foreign navies to maintain *good order at sea (* Till, 2004) (including fighting piracy) in the HoA constitutes a military dimension to achieving maritime security.

THE MARITIME STRETCHES OF THE HOA AND PIRACY INCIDENCE

The HoA's maritime domain juts out between the Indian Ocean and the Gulf of Aden, overlooking the narrow Strait of Bab el-Maneb and of the Red Sea stretching northwards, towards the Suez Canal and the Gulf of Aqada (Osifeso, 1984). In particular, the Gulf of Aden is a key maritime trade route, where thousands of ships navigate the Red Sea before passing through the Suez Canal which links Europe to Asia. Nearly 12 percent of the world's petroleum passes through the Gulf of Aden.

The region encompasses the countries of Djibouti, Eritrea, Ethiopia and Somalia. It covers approximately 2,000,000 km² and is inhabited by about 90.2 million people. The HoA's waters are strategically important for maritime transportation, especially oil-based trading given its proximity to the rich Persian Gulf region which contains half of the world's oil.

The coast of Somalia is the most strategic given its location (empties into the Gulf of Aden and Indian Ocean) and size (about 3,025 kilometres coastline). As shown in Figure 2 below, the northern coastline of Somalia lies to the south of the Gulf of Aden, a key waterway for ships transiting through the Red Sea and the increasingly active port of Djibouti. Also south-east coast of Somalia connects to the Indian Ocean waters, which are home to busy shipping lanes for trade between Asia and East Africa, as well as for ships making longer voyages around South Africa's Cape of Good Hope (Ploch et al., 2009).

Since 2005, the HoA's waters (Somali coast and Gulf of Aden) have become the most dangerous hotspot of piracy. The lastest IMB annual report shows that 2009 is the third successive

Figure 2. Map of Africa Showing Pirates Hotspots, including the Horn of Africa.

Source: Authors' elaboration

year that the number of reported incidents worldwide have increased with 239, 263 and 293 incidents reported in 2006, 2007 and 2008 respectively (IMB, 2009). The report shows that in 2009, a total of 406 incidents of piracy and armed robbery against ships were reported worldwide. Africa accounted for the highest incidence with 264 cases, and was followed distantly by South Asia with 45 cases. The Indian sub-continent recorded 39 cases, while America and Far East Asia witnessed 37 and 23 attacks, respectively. Some waters grouped as the 'Rest of the World' (ROW) recorded 8 cases of which Somali pirates are also responsible for most attacks included here.

The 2009 report reveals that worldwide, 153 vessels were boarded, 49 vessels were hijacked, 84 attempted attacks and 120 vessels fired upon – compared to 46 ships fired upon in 2008. A total of 1052 crew were taken hostage, 68 crew were injured in the various incidents and 8 crew killed. Statistics in Figure 3 shows that the incidence of piracy off the HoA has been on the increase since 2006, and Somali pirates are responsible for growing attacks in the Gulf of Aden. The situation has worsened in the last two years, and pirate attack is spreading to new areas.

Figure 3. Reported Cases of Pirate Attacks in Africa, including off the HoA, 2003-2009.
(The waters of 22 African states)

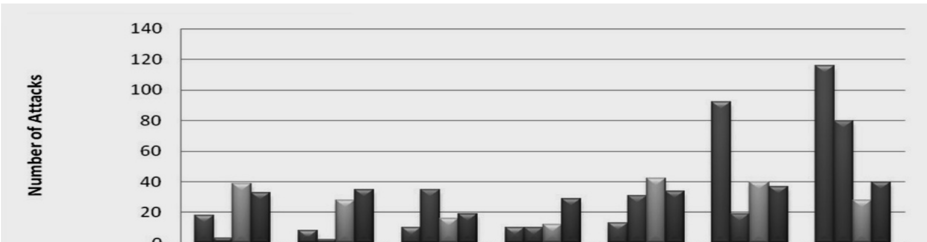

	2003	2004	2005	2006	2007	2008	2009
Gulf of Aden	18	8	10	10	13	92	116
Somalia	3	2	35	10	31	19	80
Nigeria	39	28	16	12	42	40	28
Rest of Africa*	33	35	19	29	34	37	40

Source: Adapted from IMB Annual Reports for 2008 and 2009

The IMB received a total of 217 incidents carried out by suspected Somali pirates in 2009. A total of 47 vessels were reported hijacked and 867 crewmembers were taken hostage. A further 10 were reported injured, 4 killed and one missing. Further breakdown shows that the attacks included 80 off the east and south coast of Somalia, 116 in the Gulf of Aden, 15 around the southern Red Sea, 4 off Oman, 1 in the Arabian Sea and another 1 in the Indian Ocean. Somalia accounted for more than half of the 2009 figures, and their targets have included bulk carriers, containers, fishing vessels, tankers, tugs, and yachts.

Further, 2009 recorded a significant shift in the area of attacks off Somalia. While the 2008 attacks were predominantly focused in the Gulf of Aden, 2009 witnessed more vessels also being targeted along the waters off the east and south coast of Somalia, including the Indian Ocean, Gulf of Aden, Southern Red Sea, Straits of Bab El Mandeb, off east coast of Oman and the Arabia Sea. Many of these attacks have occurred at distances of approximately 1000 nautical miles off Mogadishu.

While the number of attacks in 2009 had almost doubled, the number of successful hijackings is proportionately less when compared to 2008 figures. In 2008, for instance, 111 vessels were targeted by Somali pirates resulting in 42 hijackings. In contrast, Somali pirates carried out 217 attacks resulting in only 47 hijackings in 2009. This was attributed to the increased presence and coordination of the international navies coupled with growing awareness and robust action by the Masters in transiting these dangerous waters. Nevertheless, statistics in Table 1 show that worldwide, pirates are becoming more violent in their attacks in the last three years. Overall use of arms was on the decrease between 2003 and 2006. Since 2006, however, recorded use of arms has been on the increase of which 409 cases were reported in 2009.

Table 1. Types of Arms used during Attacks, January – December 2005-2009

Types of Arms	2003	2004	2005	2006	2007	2008	2009
Guns	100	89	80	53	72	139	240
Knives	143	95	80	76	67	68	70
Not Stated	168	130	103	100	110	80	90
Other Weapons	34	15	13	10	14	6	6
Total at Year end	**445**	**329**	**276**	**239**	**263**	**293**	**406**

Source: Adapted from IMB Annual Reports for 2008 and 2009

Furthermore, the level of violence towards the crew by Somali pirates has increased, along with the number of crew injuries. They are now prepared to use sophisticated weapons like Rocket Propelled Grenades at vessels in a bid to stop them. As shown in Table 2 below, over all level of violence by Somali pirates moved from 205 in 2007 to 838 in 2008. Although the figure for 2009 provided here shows modest increase to 872, in actual fact the figure is much higher if the incidents attributed to suspected Somali pirates operating off Oman is added.

Table 3. Types of Violence to Crew by Somali Pirates, 2007-2009.
(The figures recorded under Somalia and Gulf of Aden)

Type of Violence	2007	2008	2009
Assaulted	–	–	–
Hostage	177	815	857
Injured	6	2	10
Kidnap	20	3	–
Killed	2	4	4
Missing	–	14	1
Threatened	–	–	–
Total	**205**	**838**	**872**

Source: Adapted from IMB Annual Reports for 2008 and 2009

Interestingly, the motives of pirate attacks off the coast of Somalia and

Gulf of Aden since 2005 have remained largely opportunistic, geared towards ransom. Once the attack is successful and the vessel hijacked, the pirates sail the vessel towards the Somali coast and thereafter demand a ransom for the release of the vessel and crew. It is not surprising as evidenced in Figure 4 below that hostage-taking of crew account for over 90 per cent of violence recorded between 2007 and 2009.

Figure 4. Percentage Distribution of Violence to Crew by Somali Pirates, 2007-2009
(combination of the figures recorded under Somalia and Gulf of Aden)

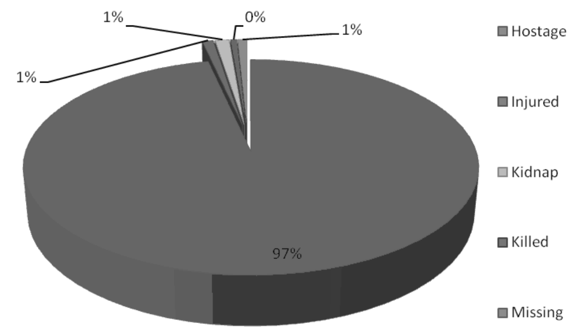

Source: The figures recorded under Somalia and Gulf of Aden

The piracy enterprise in Somalia seems to have created a window of business opportunity with network of interests involving security agents, local officials, warlords, and various foreign agents who pose as negotiators. It is alleged that the "professional negotiators are mainly retired SAS British argents or retired intelligence officers of the Australian or South African armed forces' (Ogunbayo, 2009).

The possibility that the motives for pirate attacks could move from being financial to being political in the near future is not remote given the increasing alliance between Somali pirates and the radical Islamic group, the Al Shabaab, known to have links with the Al Qaeda. Also, Al Qaeda growing presence in Yemen, known as the Al Qaeda in the Arabian Peninsula (AQAP), could further complicate the maritime insecurity picture in the region.

OVERVIEW OF FOREIGN NAVAL INTERVENTION OFF THE HOA

The deployment of foreign navies to patrol the area is one attempt to guarantee the security of merchant shipping along the Somali coast and in the Gulf of Aden, dating back to 2008. In August 2008, for instance, the US Naval Forces Central Command (NAVCENT) set up a Maritime Security Patrol Area (MSPA) in the Gulf of Aden, involving coalition navy warships and aircraft which patrols the waters and airspace of the area. Before the establishment of the MSPA, efforts were focused on Combined Task Force 150 (CTF-150), a multinational operation which patrolled the Gulf of Aden, Gulf of Oman, Arabian Sea, Red Sea and Indian Ocean and whose main aim is to counter terrorism. Its main contributors are Britain, France, Germany and the USA. However, the MSPA was and interim framework designed to counter destabilising activities in the region and improving security while long-term initiatives mature.

In January 2009, the NAVCENT established Combined Task Force 151 (CTF-151), with the sole task of combating piracy in the Gulf of Aden and the waters off the Somali coast in the Indian Ocean. Before the establishment of the CTF-151, efforts were focused on CTF-150. To further enhance collaboration among foreign navies, the US and four other nations (Britain, Cyprus, Japan and Singapore) signed onto an international plan, the “New York Declaration”, on September 2009. The non-binding declaration aims to coordinate international naval patrols, enhance shipping self-protection measures and discourage the payment of ransom to pirates operating in the region.

In mid-2008, the European Union (EU) also initiated a Close Support Protection (CSP) system for vessels passing through the Gulf of Aden. This operation involves arranging the passage of ships in groups through a special (UKMTO) transit corridor, based on their transit speed. Naval and air surveillance are deployed within the area to wade off attacks and provide support to ships. The vessels can also alert the accompanying warships for assistance if they are attacked by pirates. The NATO also floated an intervention known as *Operation Allied Protector* between October and December 2008. However, both the CSP and *Operation Allied Protector* were later integrated into the broader EU’s maritime security initiative known as *Operation Atalanta* which has been in operation since 5 December 2008.

Apart from the US and the EU, a flotilla of warships from other states such as China, Russia, Japan, Iran, among others, have intervened to protect merchant shipping in the region. Intervention by foreign navies arose partly from the need to protect their states’ economic and security interests and partly in response to the UN’s call for the suppression of acts of piracy in the area. The UN Security Council issued four key resolutions (1816, 1838, 1846, and 1851) in 2008 to enhance international response to piracy off the HoA. UN resolution 1838, for instance, calls upon ‘States whose naval vessels and military aircraft operate on the high seas and airspace off the coast of Somalia to use on the high seas and airspace off the coast of Somalia the necessary means, in conformity with international law, as reflected in the Convention, for the repression of acts of piracy’(UNSC, 2008).

The international armada assembling off the coast of Somalia created expectations of quickly suppressing the piracy threat through deterrence and intervention. However, statistical evidence from the IMB reports (2008 and 2009) show that piracy in the region has not decreased. If anything, it is increasing and spreading to new areas, and risks assuming a more ominous dimension.

EMERGING RISKS ASSOCIATED WITH FOREIGN NAVAL INTERVENTION IN HOA

The foregoing demonstrates the level of response that combating piracy off the HoA has received from the international community. Observably, naval show of force has received immediate and enormous support from the developed countries, almost to the neglect of other critical socio-economic and political measures that would help stabilize Somalia: the principal source of insecurity offshore.

Unfortunately, foreign naval intervention comes with its unintended effects or risks. What are the emerging risks associated with the intervention of foreign naval forces to enhance maritime security off the HoA? Below are some of the implications of foreign naval intervention in the fight against piracy in HoA.

Desperation and Expansion of the Range of Attacks

First, the intervention of foreign navies has added a new dimension to the desperation of Somali pirates, evidenced in the increasing resort to violence (the use more arms and the firing of sophisticated weapons) and the extension of their attacks farther out at sea. Hitherto, pirates have largely operated on the coast of Somalia and the Gulf of Aden. Figure 5 below shows that the range of attacks has expanded from just 165 nautical miles off the coast of Somalia in 2005 to about 1, 1000 nautical miles in early 2010, suggesting an increase of over 5% in six years. Yet, the range of attack is even growing. On 17 April 2010, suspected Somali pirates hijacked three Thai fishing vessels – MV PRANTALAY 11, MV PRANTALAY 12 and MV PRANTALAY 14 – in the Indian Ocean. The three vessels, carrying a total of 77 crew members, were hijacked about 1,200 nautical miles (2,222 km) from the Somali coast (BBC News, 2010).

Figure 5. Expansion of Pirates Attacks off the Horn of Africa.

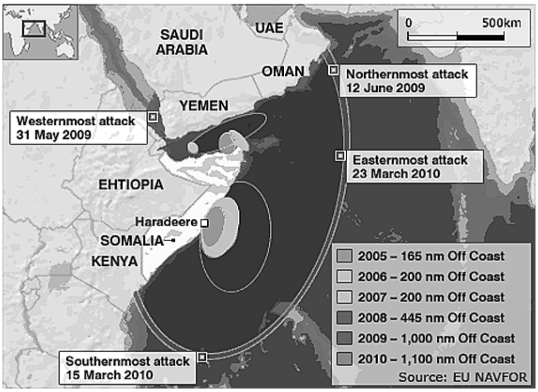

Source: Nick Childs (2010)

In contrast to the pattern of earlier years, Somali pirates now attack vessels further out at sea, including off Kenya, Tanzania, Seychelles and Madagascar. They have demonstrated the capacity of attacking vessels as far west as the southern region of the Red Sea and the Bab el Mandab Straits, and as far north as off east coast of Oman and the Arabian Sea.

Rising Stakes: Trade-by-Barter

The intervention of foreign navies has raised the stakes both for pirates and crewmembers. For pirates, it has led to higher risk of the criminal act in terms of their arrest or even killing by foreign navies. For crewmembers, it has lead to more violence as well as demand for higher ransom by pirates. Because the stakes are now high, Somali pirates appear to attach a 'conditionality' that gives them leverage over

States and their navies attempting to clamp down on piracy. This entails demand by pirates for the release of their captured colleagues (something akin to barter), in addition to ransom, in exchange for the release of crewmembers taken hostage by them. Pirates appear to have an edge in this challenge. For instance, a typical pirate raiding group usually comprises 8 to 10 men. Arrest by foreign navies has not gone beyond five pirates. But a successful pirate swoop can net in about 24 crewmembers or even more as hostages.

Propitious to Ideological Struggle

The intervention of foreign navies is propitious to ideological struggle amongst foreign navies. A sign of this is emerged following the deployment of Iranian naval warship in the Gulf of Aden to help protect Iranian ships transiting through the region. On August 2009, for instance, Deputy Commander of Iran's Islamic Revolution Guards Corps (IRGC) Navy, Brig. Gen. Ali Fadavi, relished that:

The IRGC Navy accomplished a trans-regional mission to provide security for the Iranian commercial ships in the Gulf of Aden and once again proved that it has the capability to establish security outside its geographical region....This is while, despite the presence of their advanced naval fleets, the US and European countries have failed to repel the piracy threat facing their vessels (Davet, 2008).

Iranian naval presence undoubtedly discomforts the US given the ruffled diplomatic relations between the US and Iran over the latter's nuclear programme. Consequently, the international armada of warships has been unable to suppress piracy partly because of the tendency of navies to depart when their own interests or citizens are no longer under threat or as a result of some perceived ideological differences.

Risk Exacerbating Regional Tension

One of the challenges to combating piracy borders on what happens once pirates have been caught. Any state can shoulder the burden of prosecution, although few are willing to do so. A problem arises when a state whose ship was attacked or whose navy arrested pirates but does not have existing law that criminalises piracy. Somalia for instance does not have a law against piracy. Consequently arrangements have been made by foreign navies to hand over suspected Somali pirates to the country's neighbour for prosecution.

In January 2009, for instance, the US and the UK signed a memorandum of understanding with Kenya that permits them to hand over to Kenyan authorities captured pirates for prosecution (Shinn, 2009). When captured Somali pirates are handed over to neighbours like Ethiopia and Kenya for prosecution, the tendency for resentment and hatred by Somalis may increase. Such arrangements in the future could fracture the contours of inter- and intra-state animosity in a region that is known for the complexity of its instability.

CONCLUSION AND RECOMMENDATIONS

The outbreak and continuance of piracy off the coast of Somalia and the Gulf of Aden has become a serious problem for the international community. Foreign navies have intervened to guarantee maritime security, but their presence seems to be complicating the problem. To stem the scourge of maritime piracy in the region, the following recommendations, although hardly exhaustive, are adduced.

Firstly, the international community, under the platform of the United Nations Organisation, must assume its full responsibilities in Somali, by facilitating the immediate deployment of a strong UN peace enforcement operation. Top priorities for the UN operation should include, among others, the protection of civilians, the restoration of order to pave the way for a more inclusive government in Somalia and the rebuilding of the bartered economy after the peace process. Troop contributing countries to such UN contingent must be ones without direct or indirect interest (among which include Ethiopia, Kenya, the US) in the internal dynamics of Somali politics.

Secondly, there is the need for the international community to agree on, and put in place, a central Anti-Piracy Task Force off the Horn of Africa (APTF-HoA) to lead the international efforts at suppressing piracy and maritime raiding off the HoA. Such a Task Force must be structured in a manner that demonstrates African ownership of the initiative. This requires at least two minimum criteria. First, the Commander of the APTF-HoA should come from Africa, save the East Africa region. Second, foreign navies operating along the region's coast should establish cooperative partnerships with navies of coastal states in the region (Onuoha, 2009). Without cooperation by these African coastal states it will be difficult if not impossible to legalise an isolated intervention much less a sustained systematic anti-piracy campaign in the region. This kind of initiative would serve the dual purpose of attaching legitimacy to the Task Force and offer African navies the opportunity to build their capacities for policing their waters. The scope of operation of the APTF-HoA must go beyond merely fighting piracy to include emphasis on effective protection of the marine resources of Somalia from liberal pillaging and the dumping of toxic wastes by foreign (and local) fleets.

Thirdly, the AU together with other stakeholders should intensify its collaboration with the regional economic communities (RECs) to ensure that the concepts of the African Standby Force (ASF) and the Sub-Regional Standby Brigades become functional in June 2010 as envisaged in the roadmap. This would require firstly the incorporation of a maritime dimension into the ASF's doctrinal framework for peace support operations. And second, efforts must be made through training and logistic procurement to develop the capacity of the regional brigades to protect Africa's maritime interests within a clearly defined holistic maritime security strategy for Africa.

Fourthly, there is a need for the African Union, regional organisations, national governments, civil society organisations and grass roots communities to intensify collaborative networks and strengthen mechanisms to control the proliferation and circulation of SALWs in the HoA.

Finally, achieving sustainable maritime security in Africa demands that the root causes of piracy in Africa is effectively tackled, rather than reacting to this symptom of a deeper malaise. Most security challenges confronting Africa have their origin in the progressive failure of governance and internal contradictions that serve to undermine human development and generate conflicts within states. The factors are legion, but corruption, marginalisation and injustice figure as the most prominent causes of insecurity onshore, which have now been extended offshore. Good governance is therefore absolutely fundamental to achieving sustainable maritime security and development in Africa. Hence, efforts must be made to address bad governance in African states. The importance of policies designed to curb corruption in African states, ensure transparency and accountability in the management of national resources, greater investment in human development, and the strengthening of the democratic (especially the electoral) processes to ensure the emergence of credible leaders cannot be over-emphasised.

REFERENCES

BBC News, 2010: "Somali pirates seize three Thai fishing vessels", 20 April 2010, http://news.bbc.co.uk/2/hi/africa/8632232.stm, Accessed on: 24 April 2010.

Bimbo Osifeso, 1984: "Superpower Rivalry in the African Horn", *Nigerian Forum,* 4(10, 11&12) (1984) p.255.

David Shinn, 2009: 'Rise of Piracy and other Maritime Insecurity in Somalia', (2009) Available at http://www.eastafricaforum.net/2009/04/11/rise-of-piracy-and-other-maritime-insecurity-in-somalia Accessed on: 14 May 2009.

Frank C van Rooyen, 2007: "Africa's Maritime Dimension: Unlocking and Securing the Potentials of its Seas – Interventions and Opportunities, *African Security Review,* 16(2) (2007), 112.

Freedom C Onuoha, 2009: 'Globalization, Sea Piracy and Maritime Security off the Horn of Africa', paper presented at the 9th Nigerian Sociological Society Annual Conference on *The Sociology of Globalization and the Crises of Capitalism in Nigeria*, Conference Centre, University of Lagos, Akoka, Yaba-Lagos, 24-26 November 2009.

Freedom C. Onuoha, 2009: "Sea Piracy and Maritime Security in the Horn of Africa: The Somali Coast and Gulf of Aden in Perspective' *Africa Security Review,* 18, 3 (2009), p. 33.

Geoffrey Till, 2004: *Power: A Guide for the Twenty-First Century,* (London: Frank Cass, 2004) p.310.

IMB, 2009: *Piracy and Armed Robbery against Ships: Report for the Period 1 January – 31 December 2009,* (London: IMB, 2010) p.21.

International Maritime Bureau (IMB), 1997: *Piracy and Armed Robbery against Ships: A Special Report,* (London: International Chamber of Commerce, 1997), p.2.

İslâmi Davet, 2009: "IRGC Thwarted Pirate Attacks in Gulf of Aden", *http://www.islamidavet.com/english/tag/gulf-of-aden/* Accessed on: 2 October 2009.

Lauren Ploch, 2009: Christopher M. Blanchard, Ronald O'Rourke, R. Chuck Mason, and Rawle O. King, **"**Piracy off the Horn of Africa", *Congressional Research Service* R40528 , 24 April 2009, p.10.

M Ogunbayo, 1983. 'War on Piracy: The Enemies within', *Newswatch,* 4 May 2009, p.36.

Margaret. A. Vogt, "Securing Nigeria's Territorial Waters", *Nigerian Forum,* March/April (1983), p.1039

Micheal Pugh and F. Gregory, 1994: 'Maritime Constabulary Roles of Non-Military Security', in M. Pugh (ed.) *Maritime Security and Peacekeeping: A Framework for United Nations Operations* (New York: Manchester University Press, 1994) p.83.

Nick Childs, 2010: "Navies struggle with 'swarming' Pirates", *BBC News*, 1 April 2010, http://news.bbc.co.uk/2/hi/africa/8598726.stm, Accessed 12 April 2010.

Oil Companies International Marine Forum (OCIMF), 2009: *Piracy: The East Africa/ Somalia Situation Practical Measures to Avoid, Deter or Delay Piracy Attacks*. (Scotland: Witherby Seamanship International Ltd, 2009), p.1

United Nations Convention on the Law of the Sea (UNCLOS), 1982: Article 101.

United Nations Security Council (UNSC), 2008: "Resolution 1838" (October 2008) *http://daccessdds.un.org/doc/UNDOC/GEN/N08/538/84/PDF/N0853884.pdf?OpenElement* Accessed 12 November 2008.

Journal of Maritime Research, Vol. VII. No. 3, pp. 57-70, 2010

ISSN: 1697-4840

SPEED DEFICIENCY IN SHIPBUILDING CONTRACTS FROM THE POINT OF VIEW OF THE MAIN ENGINE MANAGEMENT

I. Basterretxea[1,2], **J. Vila**[1,3], **I. Loroño**[1,4], **L. Martín**[1,5] and **M. Herrera**[1,6]

Received 18 May 2010; in revised form 21 June 2010; accepted 12 October 2009

ABSTRACT

This article is related to the shipbuilding contracts and its purpose is to provide a method of calculation of the economical damages sustained by a purchaser due to the speed deficiency of the vessel delivered by the shipyard. The method is easy to be put into practice in all types of ships because it is based on the management of the main engine and does not use economical terms which may make it confusing and volatile.

Keywords: Shipbuilding contract, propulsive power, speed contracted or agreed, speed deficiency, ship extra costs

INTRODUCTION

The speed deficiency in sale contracts of ships, either existing or new building, involves claims whose quantum is difficult to calculate due to the fluctuations of economical parameters. In case of new ships delivered by the shipyard, the damages are usually higher due to a longer lifetime.

This article aims to present an assessment method for the economical quantum of speed deficiency claim from the point of view of the main engine management. The calculation is mainly based on the excess of fuel consumption arisen from the power increase of the main engine necessary to reach the speed agreed in the ship-

[1]Professor University of the Basque Country, Maria Diaz de Haro, 68 48920 Portugalete, Spain. [2]Email: imanol.basterrechea@ehu.es, Tel. 946014792, Fax. 946017700. [3]Email: jesusangel.vila@ehu.es, Tel. 946014859, Fax. 946017700. [4]Email: inaki.lorono@ehu.es, Tel. 946017780, Fax. 946017700. [5]Email: leopoldo.martin@ehu.es, Tel. 946014119, Fax. 946017700. [6]Professor, Email: mariamercedes.herrera@ehu.es, Tel. 946014869, Fax. 946017700.

building contract. Moreover other consequences caused by a major power should be taken into account as main engine wear and tear, lube oil consumption, reduction of payload, etcetera. One of the advantages of the method is that it can involve all types of ships without using economical variables related to fluctuations of freight market, delays for arriving out of time to the ports of loading or unloading in regular lines, etcetera. Nevertheless the uncontrollable price of oil products may make the results of this method volatile.

METHODOLOGY

One of the first problems for the shipyard is that the propulsive power to reach a specific speed must be known before the sea trials are carried out. Therefore the resistances of the hull and its appendices at a specific speed must be determined in advance by statistical methods and model tests. The speed deficiency in shipbuilding contract is usually caused by an error in the calculation of the resistances for a particular speed.

On the other hand, the shipbuilding contract clauses related to the speed, power and consumption will also be considered as well as the clause called *liquidated damages* which provides the way of settling damages for speed deficiency.

In case the speed of the new vessel does not reach the speed agreed in the contract, this research will provide us with a simple method to assess the increase in fuel consumption, oil lubrication and maintenance of the main engine to reach that agreed speed, without prejudice to the main engine life.

Calculation of required propulsive power at the initial design stage of the ship

Before the construction of the ship, the ship's main particulars required by the buyer are provided to the shipyard where the basic ship design is carried out involving the calculation of the main engine power by using some of these main particulars. At this regard, both project speed and any other speed may be determined, respectively,

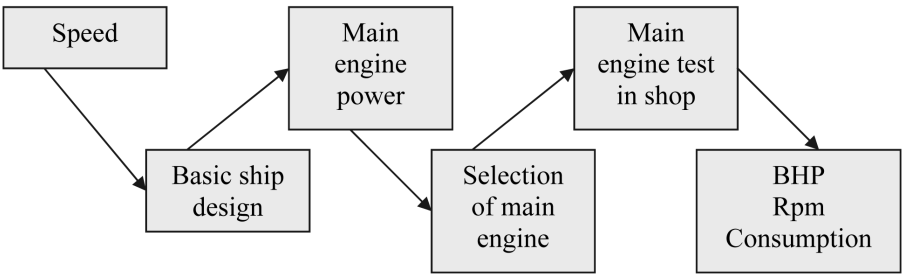

Figure 1.

by means of proximate methods as J. Mau or D.G.M. Watson and J. Holtrop & G.G.J. Mennen or L.K. Kupras. Thus the relation between the propulsive power and the ship speed may be known before the beginning of the shipbuilding and the steps taken by the shipyard are shown in figure nº1.

Once the propulsive power is assessed, a main engine is chosen by the shipyard to provide the ship with enough power to reach the agreed speed (service or maximum speed depending on the contents of shipbuilding contract). A little difference between the shop or sea trial (around 3%) is taken into account by the shipyard since the main engine works in a different way either on board the ship or in the shop.

Shipbuilding contract

The ship speed is agreed under the shipbuilding contract at a specific draught (mainly the draught in sea trials), power (BHP) and sea conditions. Sometimes a sea margin (around 15% or less) may be agreed in the contract to take into account the loss of speed caused by the sea condition (swell, waves, wind, etcetera…).

Fuel oil consumption for a given propulsive power is also agreed under the contract according to the details of the shop trials. This data can be known in advance by the shipyard by means of the results of main engine shop trial (considering the additional percentage of around 3% cited previously).

A special compensation clause for damages due to speed deficiency is usually included in the standard forms of shipbuilding contracts (SAJ, AWES, MARAD, Norwegian Shipbuilding Contract or NEWBUILCON). For instance, the BIMCO's new standard agreement says as follows:

8. Speed Deficiency

If the speed of the Vessel as stated in Box 4D(ii) is not achieved in the manner stated in the Specification or Clause 2(b)(i) the following shall apply:

(a) There shall be no adjustment of the Contract Price except to the extent provided in Sub-clause 8(b).

(b) lf the reduction in speed is greater than 2/10ths of a knot, the Contract Price shall be reduced by the amount stated in Box 13(i) for each whole 1/10th of a knot reduction in speed in excess of 2/10th of a knot as liquidated damages up to the maximum amount stated in Box 13(ii).

(c) lf the reduction in speed would entitle the Buyer to a reduction in the Contract Price greater than the maximum amount stated in Box 13(ii), the Buyer shall have the option to terminate this Contract in accordance with Clause 39(a)(iv) (Suspension and Termination).

According to this clause, the contract price is not to be reduced if the loss of speed is equal or minor to 0.20 knots in respect to the speed agreed in the contract. However the contract price will be reduced by an agreed amount for each whole 0.10

knots reduction in excess of 0.20 knots up to a maximum sum stated in the contract.

Of course, the speed deficiency may be negotiated in the contract by means of different clauses depending on the form of the agreement. There are even many shipbuilding contracts where any compensation is not agreed with regard to the speed deficiency and the disputes are finally brought before the Court.

Calculation of extra fuel consumption to reach the agreed speed

The minimum service speed agreed under shipbuilding contract is subject to a given propulsive power (BHP), vessel's draught, sea margin or whatever other condition. Under the standard form contract NEWBUILDCON, for instance, it is agreed a minimum service speed under following conditions:

- Minimum service speed at design draft
- Minimum service speed at a percentage of the main engine's maximum continuous power
- Minimum service speed at a specific consumption rate
- Sea margin

In this way, if that minimum service speed is not reached at above conditions during the ship trials, the power of the main engine may be risen up to reach it. Unfortunately this major power would mean a higher consumption of fuel oil along the ship's life which will serve us for the calculation of the compensation.

Calculation of main engine life reduction

The life of the main engine may be represented in the figure nº 2 by the bathtub curve (figure nº2) where the conditional probability of failure is related to the main engine's lifetime. During the first months of ship operation (infant mortality) the incidence of failure is high but it is followed by a constant or gradually increasing probability of failure (constant zone). Then, after several years of operation at the same minimum level, the probability of failure begins to rise in the wear-out zone due to wear and tear of the engine.

Although the shape of that curve depends on the type of engine, it may be considered in the research an average lifetime of twenty years before the wear-out zone.

The increase of power output of the main engine to reach the agreed speed

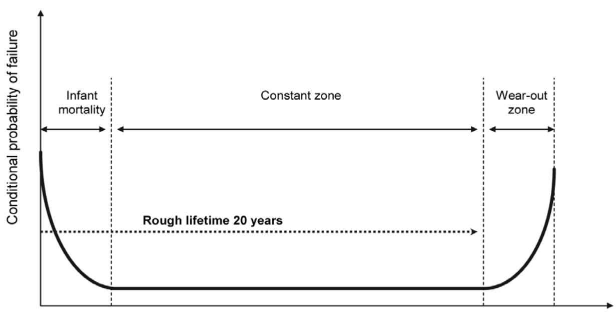

Figure 2. Bathtub curve.

entails a reduction of main engine lifetime. In order to stop this reduction, the main engine maintenance should be carried out more frequently and therefore the related costs would be higher as it will be studied in the next chapter.

Calculation of the extra cost of main engine maintenance

Higher power output involves a major wear and tear in the parts of the main engine and consequently its lifetime is reduced. To keep the same lifetime, the ship manager is obligated to carry out maintenance works during shorter periods of time which will depend directly on the difference between the power stated in the contract for the agreed speed and that power which is really needed for the ship to provide the agreed speed. A way of this extra cost calculation might be based on a percentage of main engine maintenance annual cost.

Calculation of the extra cost of lube oil consumption

The lube oil consumption would be higher in case of the main engine rate (revolutions per minute) being increased to reach agreed speed. This excess of lube oil consumption may be assessed from the real data of the main engine in service. This means to compare the lube oil consumption at the propulsive power corresponding to the agreed speed and at the power output needed for the ship to provide the agreed speed. If there would not be previous experience to obtain those data, the lube oil consumption may be considered proportional to the revolutions per minute of the main engine.

Freight loss

If the ship has to consume more fuel to reach the agreed speed, the fuel loaded in her tanks to keep the same sea passage range would be greater and consequently the payload would be reduced. This loss of cargo would mean a lower freight for the same sea passage.

PRACTICAL CASE

This method of calculation for damages caused by speed deficiency under shipbuilding contract is put into practice on an existing oil tanker of 150,000 dwt. The research will be carried out for a speed deficiency of 0.1 knots between the contractual and real service speed once the allowance is taken.

Specifications of the contract

The shipbuilding contract is agreed according to the following guarantees:

- 150,000 tons deadweight SUEZMAX oil tanker
- Specified speed without sea margin at the condition of clean bottom in sea trial condition within Beaufort 2:

- 16.2 knots at the mean summer draught of 16 meters and at 90% MCR (14.560 kW) of main engine.
- 16.8 knots at the mean ballast draught of 7 meters and at 90% MCR (14.560 kW) of main engine.

— Settlement of damages: If the deficiency in actual speed of the vessel amounts to or exceeds two-tenths of one knot below the specified speed of the vessel at the design draught, the Builder shall pay compensation to the Buyer for the excess speed deficiency.
— Maximum Continuous Rating (MCR): approx.16.178 KW
— Normal Continuous Rating (NCR = 90% MCR): Approx. 14.560 kW
— Consumption of fuel oil guaranteed (at NCR): 173,07 g/kW/h.

Data collecting from sea and shop trials

The result of sea trials with the ship loaded at summer draught of 16 meters is shown in table 1.

Vessel at maximum loaded condition	75% MCR	NCR (90% MCR)	MCR
Corrected speed (knots)	14.97	15.9	16.31
BHP (kW)	12,133	14,560	16,178
Consumption (g/kW/h)	173.76	173.07	175.66

Table. 1.

In addition, the outcome of these trials at ballast draught of 7 meters is shown in table 2.

Vessel at ballast condition	75% MCR	NCR (90% MCR)	MCR
Corrected speed (knots)	15.6	16.6	17.5
BHP (kW)	12,133	14,560	16,178
Consumption (g/kW/h)	173.76	173.07	175.66

Table. 2.

Data collecting from the ship in service

The following data are collecting from the ship's experience along her life:
— Navigation time: 264 days per year
— Navigation time at summer draft: 158 days per year
— Navigation time at ballast condition: 106 days per year

— Lubricating oil consumption of main engine at BHP 14,560 kW (NCR): 715 liters per day
— Lubricating oil consumption of main engine at BHP 14,925 kW: 725 liters per day
— Cost of main engine's maintenance:
  - Spares: 45,000 annual USD
  - Cost of repairing and maintenance works: 25,000 annual USD
— Average freight: 24,000 USD per day

Extra cost of fuel consumption

The speed of 16.9 knots with the ship sailing at maximum condition load and at 90% MCR is 0.1 knot below the agreed speed, once deducted two tenths of a knot allowance. On the other hand, the speed at ballast condition is considered within the agreed parameters.

The full relationship between power, speed and consumption is shown in table and figure nº 3 and obtained from the real data of the sea trials (shown in table nº 1 and in bold in table nº 3) by using *spline* interpolation. It is also marked within a double cell the minimum agreed speed along with the power and related consumption.

BHP (kW)	**11.881**	12.023	13.585	13.889	14.214	**14.560**	14.925	15.311	15.718	16.145	**16.178**	16.592
SPEED (KNOTS)	**14,8**	14,9	15,6	15,7	15,8	**15,9**	16,0	16,1	16,2	16,3	**16,312**	16,4
CONSUMPTION (kg/h)	**2.068,0**	2.090,4	2.352,2	2.404,5	2.460,3	**2.519,9**	2.583,0	2.650,6	2.730,2	2.833,0	**2.841,8**	2.959,4
CONSUMPTION (g/kW/h)	**174,06**	173,87	173,15	173,12	173,09	**173,07**	173,07	173,12	173,70	175,47	**175,66**	178,36

Table 3.

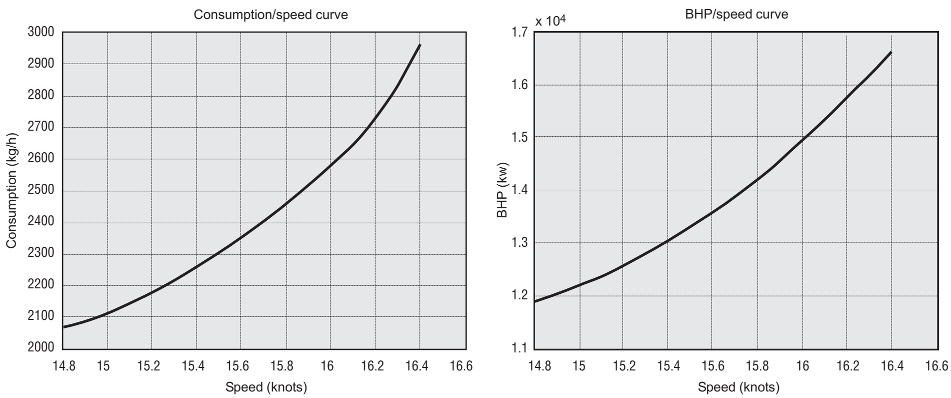

Figure 3.

As it is shown in table nº 3, consumption between real speed of 15.9 knot and agreed speed of 16.0 knot (deducted allowance of 0.2 knots) is increased in 63.1 kg/h (from 2,519.9 kg/h to 2,583.0 kg/h). Bearing in mind a yearly navigation time in loading condition of 158 days, consumption would be increased in 239,275 kg per year. If an average fuel price of USD 0.40 per kilogram is considered along 20 years, the extra annual cost of fuel would be 95,710 x 20 = 1,914,202 USD. However, this figure should be taken into account as an approximation since the fuel price is difficult to determine in future due to the volatile oil products prices as it is shown in figure nº 3.

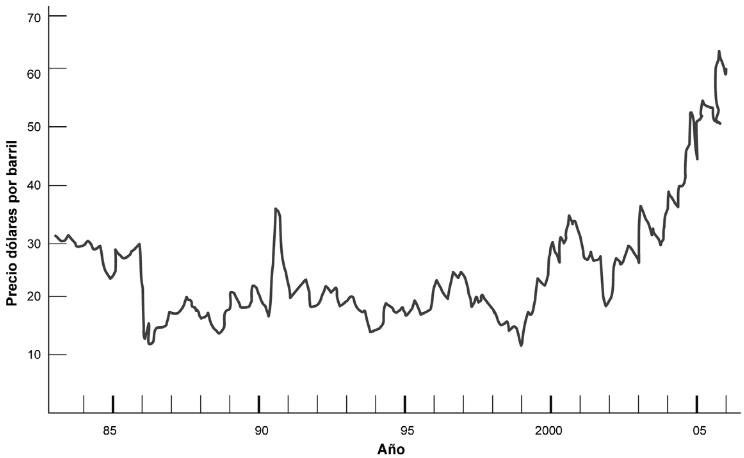

Figure 3. Price evolution of crude oil barrel along last twenty five years.

Extra cost of lubricating oil consumption

When the power of main engine is raised to reach the agreed speed, the lube oil consumption is increased in the same proportion of the engine revolutions. According to the data obtained from the ship full loaded sailing at 16.0 knots, the lube oil consumption is 10 daily litres higher than at 15.9 knots. Therefore the annual increase of lube oil price is estimated in 1.4% [100 x (10 ÷ 715) = 1.4%] and equal to 1,580 litres in 158 days per year at maximum cargo condition.

The lube oil products´ price is mainly dependent on their own additives and is not coming from the crude oil, therefore it is not so volatile as fuel oil and an annual price increase of 3% may be considered based on the inflation rate. For a current price of 1.35 USD per litre, the lube oil extra cost may be assessed as follows:

$$1{,}580 \times 1{,}35 \times \sum_{0}^{n-1} (1.03)^i$$

; where n is the main engine life in years.

In case of 20 years life, the extra cost would be 57,314 USD.

Extra cost of main engine maintenance

According to the experience of the ship managers, the vessel has to carry out an average of three maintenance works per year which means 60 maintenance works in twenty years. Taking into account that the BHP is increased from 14,560 kW (speed 15.9 knots) to 14,925 kW (speed 16.0 knots) in order to reach the agreed speed and, although it is difficult to know exactly how the components of the main engine are worn out, it might be estimated a 5% reduction in the time elapsed between two consecutive maintenance works. In this way, ship managers would need 84 days in order to operate the vessel at agreed speed. In economical words, the engine maintenance cost would also rise by 5% per year and therefore the extra cost would be 70,000 x 20 years x 5% = 70,000 USD.

Freight loss

Assuming the passage at maximum load condition is an average of 15 days long, the payload of the vessel (estimated in 143,000 tons) would be reduced in 22.7 tons [63.1 kg/h x 24 x 15] which means a percentage of 0,016% (100 x 22.7 ÷ 143,000). Taking into account the freight pays for a day according to the worldscale index, an average daily freight of 24,000 USD per day would be reduced in 3,84 USD per day, that would be around a loss of 15,000 USD in 20 years. Nevertheless the loss in payload might be absorbed by the crude oil API or even by the constant itself.

CONCLUSIONS

This calculation method may be useful to determine the quantum of liquidated damages for speed deficiency clause in shipbuilding contracts.

- The variables in the calculation are reduced basically at the fuel oil price only.
- The disadvantage of the calculation is the uncontrollable variation in the evolution of the fuel oil price for the next twenty years which involves a larger difference in the quantum of the claim for speed deficiency.
- The data used in the calculation is obtained from the main engine shop tests and its previous knowledge makes the calculation easier consequently.
- The extra cost in main engine maintenance might be studied more deeply through a regression analysis of statistical results of different engines working between the normal (NCR) and maximum continuous rating (MCR).

REFERENCES

García Garrido, S. (2008: *Operación y mantenimiento de centrales de ciclo combinado.* Madrid: Díaz de Santos.

Moubray, J. (1997): *Reliability-centered maintenance*. New York: Industrial Press Inc.

Evans, J.J. and Marlow, P.B. (1990): *Quantitative methods in maritime economics*. London: Fairplay.

Laurence, C.A. (1984): *Vessel operating economies*. London: Fairplay.

Holtrop,J. and Mennen, G.G.J. (1982): An approximate power prediction method. *International Shipbuilding Progress*, July 1982

Kupras, L.K.: Optimisation method and parametric study in precontracted ship design. *International Shipbuilding Progress*, May 1971.

Watson, D.G.M.: *Practical ship design*. Oxford: 1998

FALTA DE VELOCIDAD EN LOS CONTRATOS DE CONSTRUCCIÓN DE BUQUES DESDE EL PUNTO DE VISTA DE LA GESTIÓN DEL MOTOR PRINCIPAL

INTRODUCCIÓN

La falta de velocidad en los contratos de compraventa de buques, tanto existentes como de nueva construcción, conlleva reclamaciones cuyo importe es difícil de calcular debido a las fluctuaciones de parámetros económicos. En caso de nueva construcción, los perjuicios causados suelen ser mayores debido a que su vida es más amplia.

La intención de este artículo es presentar un método de evaluación del importe económico que supone la falta de velocidad desde el punto de vista de la gestión del motor principal. El cálculo está basado principalmente en el exceso de consumo de combustible que generaría el aumento de potencia necesario para alcanzar la velocidad pactada en el contrato de construcción del buque. Además se tienen en cuenta otras consecuencias de este aumento de potencia como pueden ser el mayor desgaste del motor, el mayor consumo de aceite, la pérdida de porte, etc. Una de las ventajas del método es que puede ser aplicable a todo tipo de buques sin usar variables económicas relacionadas con fluctuaciones del mercado de fletes, retrasos en puerto por no llegar a tiempo en líneas regulares, etc. Sin embargo, la falta de control sobre el precio de los combustibles derivados del petróleo puede provocar resultados volátiles en la aplicación de este método.

METODOLOGÍA

Cálculo de potencia en el diseño básico del buque

Antes de la construcción del buque, el armador informa de las características principales que desea para su buque, siendo el astillero quien desarrolla un proyecto inicial a fin de conocer, entre otros parámetros, la potencia del motor. En este sentido, para calcular la potencia propulsora se pueden utilizar los métodos aproximados de J. Mau y D.G.M. Watson para una velocidad de proyecto, o bien los métodos de J. Holtrop & G.G.J. Mennen y L.K. Kupras para cualquier velocidad (fig. nº 1).

Posteriormente se encarga el motor que proporcione esa potencia con un consumo de combustible en servicio que variará en un pequeño porcentaje con respecto a las pruebas en banco (aproximadamente 3%).

Contrato de construcción

La velocidad se pacta en el contrato de construcción en base a un calado determinado (el que se utilice en las pruebas de mar), un régimen de potencia y unas condiciones atmosféricas determinadas. También se puede pactar unos márgenes en porcentaje de aminoración de la velocidad debido al oleaje, viento y tiempo transcurrido (denominado *sea margin*).

También se pacta el consumo de combustible a determinado régimen de potencia que el astillero puede conocer de antemano de acuerdo con las pruebas de motor en banco, incluyéndose el porcentaje adicional que se comenta en el apartado anterior.

Los contratos de construcción estándar (SAJ, AWES, MARAD, Norwegian Shipbuilding Contract ó NEWBUILCON) tienen una cláusula especial de indemnización por daños y perjuicios debido a la falta de velocidad.

Normalmente el importe de indemnización se calcula por cada décima de nudo de deficiencia hasta un máximo por encima del cual el contrato se podría rescindir. Asimismo se concede una falta de velocidad de gracia de 0,2 nudos normalmente por debajo de la cual no existe indemnización.

Por supuesto, existen otras muchas modalidades de pactar esta falta de velocidad dependiendo del contrato estándar de que se trate o del propio acuerdo que alcancen las partes al respecto. Incluso existen muchos contratos donde no se pacta ninguna indemnización y, por tanto, las reclamaciones por falta de velocidad se resuelven en los Tribunales o en la Cámara de Arbitraje.

Cálculo de consumo extra de combustible para llegar a la velocidad pactada

En el contrato se pacta una velocidad de servicio mínima correspondiente a un calado y una potencia determinada. Por ejemplo, el contrato estándar NEWBUILDCON establece una velocidad mínima de servicio a un calado de diseño y a un porcentaje de la potencia de salida del motor (*Maximum Continuous Range*) incluyendo, asimismo, el consumo a esa potencia y velocidad. De este modo que, si existe una deficiencia en la velocidad, podemos aumentar la carga del motor para llegar a la velocidad pactada. Ello supone un aumento del consumo que nos servirá para el cálculo de la indemnización.

Cálculo del coste extra de mantenimiento del motor

Un régimen más elevado de potencia supone disminuir el tiempo de los intervalos entre las revisiones para el mantenimiento del motor. Ello conlleva una disminución de la frecuencia temporal tanto en el cambio de piezas como en la realización de trabajos de mantenimiento. Asimismo, esta frecuencia dependerá de la diferencia entre ambas potencias: la contratada y la necesaria para proporcionar la velocidad pactada. Este dato debería estimarse como un porcentaje en base al coste anual de mantenimiento del motor principal.

Cálculo del coste extra de consumo de aceite

El aumento de aceite que supone el incremento de potencia puede obtenerse de la propia experiencia del motor en servicio. Para ello se comparan los consumos al régimen de potencia pactado y a la potencia necesaria para proporcionar la velocidad pactada. Si no existieran datos sobre la experiencia previa, el aumento de consumo de aceite puede considerarse proporcional al aumento del número de vueltas del motor.

Pérdida de flete

Si el buque consume más combustible para llegar a la velocidad pactada, la cantidad de combustible necesaria para mantener la misma autonomía del viaje se incrementa con la consiguiente reducción en el porte del buque al inicio del viaje. Esta pérdida será proporcional al tiempo y/o distancia del viaje marítimo y conllevaría una pérdida de flete que, a veces, puede ser absorbida por diferencias en el API si se trata de petroleros.

CONCLUSIÓN

Este método de cálculo puede ser útil para calcular el importe de la cláusula *liquidated damages* de los contratos de construcción de buques, que determina los perjuicios económicos causados por la falta de velocidad del buque.

Las variables del cálculo son reducidas básicamente al precio del combustible.

La desventaja del cálculo son el desconocimiento de las posibles fluctuaciones que sufrirá el precio de los combustibles derivados del petróleo durante los veinte años venideros.

Los datos empleados en este método se obtienen de las pruebas en banco del motor principal y su previo conocimiento hace el cálculo mas sencillo.

El coste extra en el mantenimiento del motor principal podría estudiarse en profundidad a fin de obtener una curva de regresión basada en los resultados y datos estadísticos de motores similares trabajando a diferentes regímenes de potencia.

Journal of Maritime Research, Vol. VII. No. 3, pp. 71-82, 2010
Copyright © 2010. SEECMAR

Printed in Santander (Spain). All rights reserved
ISSN: 1697-4840

A STUDY OF THE RISKIEST POINTS IN FRONT OF AN OIL SLICK DUE TO AN ACCIDENT IN THE SPANISH MEDITERRANEAN COAST

F. X. Martínez[1,2] and **A.V. Esparza**[1,3]

Received 2 July 2010; in revised form 17 July 2010; accepted 7 November 2009

ABSTRACT

Pollution from shipping traffic poses a real risk to the Spanish coast. Memories of the Fedra bulk carrier disaster in the Strait of Gibraltar, the Prestige sinking in Finisterre or the Castor near accident off Almeria coast are still fresh. The main objective of this paper is to analyse, identify and quantify the Spanish Mediterranean coastal areas where spills from tankers are most likely to occur. The article is based on a study which uses a set of variables such as geographical peculiarities, climate, ship age and traffic density to feed an algorithm. This objective function weighs these parameters all along the coast and identifies the Spanish coastal areas having the highest risk of spills.

Keywords: Pollution, western Mediterranean, spill evolution

INTRODUCTION

The Mediterranean Sea covers an area of 2.5 million km^2, which is 5 times the area of Spain. Its east-west extent is approximately 3,800 km while its average north-south extent is 800 km. Its basin has a volume of 3.7 million km^3 with an average depth of 1,500 km, a value significantly lower than the ocean's average. The Mediterranean Sea is connected to the Atlantic Ocean by the Strait of Gibraltar, which is about 14 km wide and 300 metres deep. From a hydrological point of view, other secondary passes connect with the Black Sea and the Indic Ocean through the Red Sea. Geo-

[1]Universitat Politècnica de Catalunya, Tel. +34934017920, Fax. +34934017923, Pla de Palau, 18 08003, Barcelona, Spain. [2] Titular professor, Email: fmartinez@cen.upc.edu. [3] PhD candidate, Email: amableesparza@hotmail.com.

graphically speaking, we can identify two clear basins connected by the Strait of Sicily called Eastern and Western Mediterranean.

The Mediterranean basin (particularly the north coast) is identified by limited agricultural, forest, cattle and even fishing resources, including energy, but also by large reserves of natural gas and hydrocarbons on the south coast. In a parallel sense, there is a population of 500 million people and about 300 million tourists are expected to visit the region annually during this decade. In addition, most of the main hydrocarbon export ports are located in Libya, the Mediterranean country with the largest reserves. Also worth mentioning are the port of Marseilles (French coast), the biggest import port in terms of volume, with overall annual imports of 65 million metric tons, and the three main ports of hydrocarbon traffic, located in Italy, with an added volume of 90 million metric tons.

From an internal point of view, the Mediterranean hydrocarbon traffic routes go north- south- and east-west, but we should add crude oil traffic in transit, which accounted for 421 million metric tons in 2006, from which 72 million were transported between non-Mediterranean ports (UNCTAD, 2007).

Source: www.shipphoto.net

Figure 1. Crude oil tanker MT Venture spirit in Hong Kong, 2003.

THE LEGAL SCENARIO

Such traffic intensity has sometimes had disastrous consequences in the form of spills. An example occurred in 1967 when the Torrey Canyon spilled 120,000 tons of oil after striking a reef off the coast of Cornwall, England. The incident raised awareness among the international community about the severity of accidents involving ever-larger tankers. From a historical perspective, since 1970 the number of accidents and associated volume of spills has decreased globally by about 86%, probably due to the enforcement of the MARPOL 73/78 convention (IMO, 1978), OPA 90 (DoT, 1990) and ISM Code (IMO, 1996). The number of spills used to be directly related to the volume of oil transported. However, this has changed in recent years because crude oil exchanges have increased but the amount of spilled oil has proportionally decreased.

Analysis of spills in the last four decades has revealed that most occurred during routine tanker operations at ports or terminals. The volume of oil spilled in operations has declined and 90% of spills are less than 7 tons whereas 86% of accidental spills (due to collisions or stranding) resulted in the loss of 700 tons. Among the most disastrous are Torrey Canyon in 1967, MT Jakob Maersk in 1973, MT Urquiola in 1976, MT Amoco Cádiz in 1978, MT Castillo de Bellver in 1983, MT Exxon Valdez in 1989, Aegean Sea in 1993, MT Erika in 1999 and MT Prestige in 2010.

Nevertheless, as said above, awareness of the problem has simultaneously grown, also in the Mediterranean community as it witnesses the degradation of its own sea. In 1969, the CGFM (General Comission of Fishing) of the FAO (UN) and the CIECM (Intergovernmental Oceanographic Comission) met in a working group and in 1972 a report considered the first complete study on Mediterranean pollution was issued. According to this document, hydrocarbon spills at sea (Cantano, 2004) can be classified based on their origin (see Table 1).

Table 1. Causes of accidents involving spills up to 2004.

Causes	Average
Natural	10%
From shore	64%
Tanker operations	7%
Accidents	5%
Oil rigging at sea	2%
Other than tanker ships	12%

Source Own based on Cantano, A.

It is widely known that the Mediterranean Sea is one of the most polluted areas in the world due to hydrocarbons spills, with almost half a million tons of spilled oil annually compared with the estimated world volume of 3.2 million tons. It is worth noting, however, that the Mediterranean represents only 1% of the world's sea water while its shipping traffic is 30% of the total international traffic.

The 1976 Barcelona Convention established the protection of the Mediterranean Sea against pollution by application of the UNEP (United Nations Environment Programme). In June 1995, the convention and its name were modified, and additional protocols were adopted. In 1993, Spain ratified the 1990 International Convention on Oil Pollution Preparedness, Response and Co-operation (OPRC 90). The protocol on Preparedness, Response and Co-operation to Pollution Incidents by Hazardous and Noxious Substances was approved in 2000 (OPRC-HNS Protocol) but entered in force in June 2007. MARPOL 73/78, the strongest pillar of international regulations on ship pollution prevention, had its first steps in November 1973, accumulating up to 20 amendments. The last part to enter into force was Annex VI, in May 2005.

At a national level, we should note the National Contingency Plan for Accidental Marine Pollution passed by an order communicated on 23 February 2001, which was followed by other autonomic or regional contingency plans for the Mediterranean littoral. More generally speaking, in the last four decades fighting mechanisms against sea pollution have improved, residue recovery being still one of the most important problems to solve. Moreover, new technologies such as air patrols or satellite surveillance which, together with dispersion models, help predict the evolution of oil slicks, are being incorporated into spill detection and tracking.

THE OPERATIONAL SITUATION

Hazardous goods traffic is particularly intense in “longitudinal routes” such as the Suez – Gibraltar and Bosphorus cases and in “latitudinal routes” like those connecting the North of Africa and the petrochemical complexes on the European coast, mainly in Italy, France and Spain. Freight identification is not a problem today because of unified and electronic data transmission systems like EDI manifests, Unified Customs Declaration, and specifically related to ship safety, the AIS system and the new LRIT, (IMO, 2008) in force as of 1 January 2010 and almost at 90% penetration now. 70% of Euro-Mediterranean traffic occurs in Spanish waters. In order to reduce density-related risks, the OMI has approved several Traffic Separation Schemes (TSS), e.g. for the Strait of Gibraltar in 1968, off Cabo Gata in 1998 and off Cabo Palos and Cabo Nao, both in 2002. According to data from the Spanish State Ports Agency, oil refinement activity in Spanish port terminals is now at maximum level. Nonetheless, the number of tankers calling at port is lower compared with the 1980’s because of the growing size of ships. In addition, the use of the oil pipeline network by the Compañía Logística de Hidrocarburos (CLH) led to a reduction in coastal traffic in the early 90’s. However, this trend was reversed towards the end of the decade due to an increase in consumption and the saturation of Spanish oil refinement capacity.

Figure 2. Traffic in the Alboran Sea at 08:13 GMT on 28 July 2009.

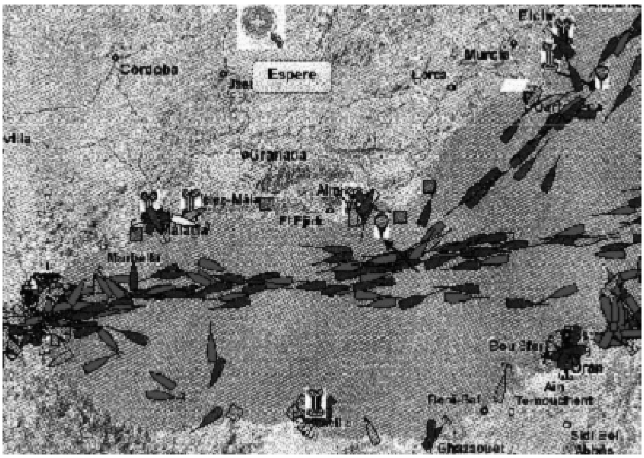

Source: www.localizatodo.com

The main routes served by tankers were analysed with 2006 and 2007 data from the Spanish State Ports Agency. The results are presented in the following table:

Table 2: Oil traffic volumes in Spanish waters.

Corridor	Hydrocarbons or derivates, traffic	Rate
Alboran Sea/Strait of Gibraltar	19,194,581	29.39 %
Spanish Med., Gulf of Lyon, Genoa	6,515,835	9.98 %
Subtotal Spanish coast	*25,710,416*	*39.37 %*
Arcew –Tarragona, Castelló	5,757,334	8.82 %
Arcew – South of Spain	433,076	0.66 %
Skikda	346,805	0.53 %
South-Western Italy	755,094	1.16 %
East-West	31,763,107	48.64 %
Balearic Islands	534,766	0.82 %
Total	65,300,600	

Source Own, based on Ports Authority data.

METHODOLOGY OF STUDY

In order to obtain a risk value for Spanish coastal areas, several parameters, like maritime traffic and climate, coastal morphology and fleet age, were chosen for the study.

Figure 3. Main hydrocarbon transport routes calling at the main Spanish Mediterranean ports.

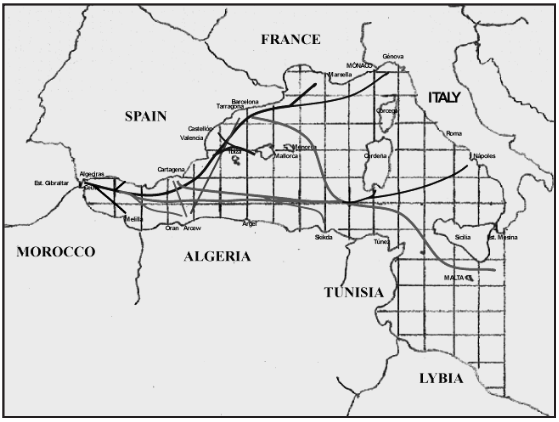

Source Own, based on Ports Authority data.

Shipping traffic in the Mediterranean Sea, and especially the East-West axis, is particularly intense. In 2006, up to 4,224 tanker shipments carrying 421 million metric tons of crude oil were reported, as opposed to 457 shipments in non Mediterranean waters, which accounted for 72 million tons in transit (REMPEC, 2008).

With 34% of berthings, the ports in the Strait of Gibraltar area have the largest number of tanker calls in the entire Spanish port system, followed by Tarragona and Barcelona with 20% and 16%, respectively. The number of calls at the Strait area is expected to exceed 4,000 within a year since 105,954 ships crossed the Strait in 2007. In 2006, 19% of ships in transit through the Strait of Gibraltar were tankers, accounting for 32% of the total tonnage. In order to have a geographical distribution, we divided the Mediterranean into squares and assigned them a risk rate from 0 to 10 depending on the volume of traffic occurring in the area.

The wind and wave regimes were also analysed with data from REMRO, XIOM and HIPOCAS projects. Data of most Eastern zones were obtained from the "Instituto Superiore per la Protezione de la Ricerca Ambientale" through its Rete Ondametrica Nazionale - RON. On the other hand, the information related to the Libya Sea was obtained from the EuroWeather-Meteomed, Mediterranean marine forecasts. Scores were given based on the average significant wave height data.

Figure 4. Risk weight for all Spanish Western Mediterranean areas.

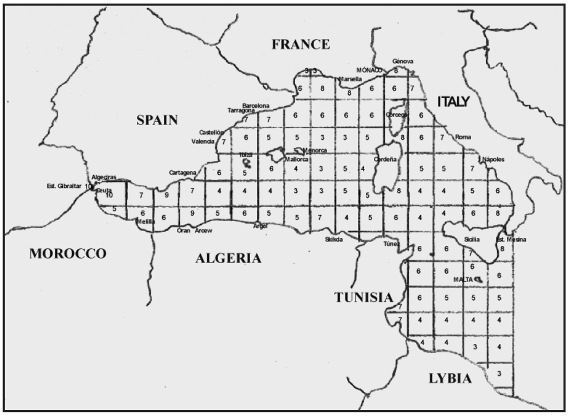

Source Own, based on Ports Authority data.

The third main parameter was Western Mediterranean morphology. Nautical and bathymetric charts gave depth information, together with other secondary data. Finally, fleet age was analysed as it is one of the factors affecting accidentability and probability of ship malfunction. In the last decade, fleet age has decreased drastically. For example, tanker age dropped by approximately 32.7%, with an average age of 10 years. In developed countries, tankers were newer, with an average age of 7.7 years in January 2007. About 70% of crude oil that crossed the Mediterranean Sea was carried on board tankers younger than 10 years old and only 4% exceeded the age of 20 years. A collateral factor to ship age is the registry flag. The analysis of tanker flags shows that 65% of cargo capacity of tankers calling at the main Spanish Mediterranean ports is from western countries and less than 10% is under third countries' flags. It should be born in mind that some convenience flag vessels are managed by western owners who choose this flag for cost or fiscal reasons only. The ports of Tarragona and Escombreras in Cartagena, which boast refineries of the Spanish company Repsol YPF, receive approximately 56% of cargo capacity under western flags. About 81% of carried hydrocarbons is moved by tankers not directly related to oil companies or states since oil the former sold their fleets some time ago.

PRELIMINARY RESULTS

After examining the four main risk factors, we calculated the risk point census. The weighting factor of each parameter was obtained from questionnaires sent to several relevant stakeholders in the maritime sector. The results were 60% to traffic, 15% to waves, 10% to morphology and 15% to fleet age. After applying the suggested weights to each area, the six points in the following table were identified as the riskiest in the Western Mediterranean.

Table 3: Weighing of the most risky areas in the Western Mediterranean.

	Strait of Gibraltar	Cape of Gata	Ceuta	Algeria Arcew	Sardinia	Marseilles
Traffic	6.00	5.40	6.00	5.40	4.80	4.80
Climate	0.75	0.90	0.60	0.45	1.05	0.90
Morphology	0.70	0.80	0.10	0.70	0.80	0.70
Fleet age	0.90	0.90	0.90	0..75	0.60	0.60
TOTAL	**8.35**	**8.00**	**7.60**	**7.30**	**7.25**	**7.00**

The affectation potential risk of the Mediterranean littoral is closely related to the prevalent wind and current in each area of study. This means that oil slicks will be affected by the weather conditions, and therefore the weather forecast for the area should be considered. This is, however, out of the scope of this paper.

Wind values in the Mediterranean area were recorded by a network of deep water buoys (REDEXT net) and meteorological stations (REMPOR net) placed at fixed positions. Wind intensity and direction were measured daily at time intervals of one hour on a long term basis. In this way, both instantaneous information and long term data can be obtained. For the riskiest points in the Spanish Western Mediterranean, the annual average wind speed was calculated with the origin data from the above web sites and the Spanish State Ports Agency.

Mediterranean currents mainly develop on the surface and are caused by the action of the wind. Nevertheless, there exists another current resulting from the difference in density of Atlantic and Mediterranean waters which circulates anticlockwise, flowing eastwards off the coast of northern Africa from the Strait of Gibraltar up to Port Said on the Egyptian coast. There, it turns north off the coasts of Israel and Lebanon and flows further to the west.

The set of currents was obtained from the Oceanographic section of the Spanish State Ports Agency, the Mediterranean Sailing Directions or Pilot Books and web sites like www.poseidon.hcmr.gr, www.meteofrance.com, www.hidromare.it, *www.eurometeo.com* and *www.freemeteo.com*. Wind and current data were classified according to the average movement of an oil slick advancing at 3% of the surface wind speed (IMO, 2005). The average speed of movement of an oil slick was calculated by an approximate formula that combines wind speed and direction effect with the existing current, as shown in the following table.

Table 4: Approximate speed of movement of an oil slick in some Western Mediterranean areas.

Geographical areas	Speed in km/h
Strait of Gibraltar	9.307
Cape of Gata	5.225
Arcew (Algeria)	3.001
Marseilles	3.958

Speeds of movement and directions of oil slicks were estimated for winter and summer, which gave different values of, for example, the time required by slicks to reach the coast.

CONCLUSIONS

International tanker fleets have been renewed in recent years. In OCDE countries, the tanker fleet had an average age of 7.7 years while the world's average was 10 years, that is, slightly higher than that of container carriers.

New ballast management, tank cleaning and residue recovery technologies, among others, have improved operational safety and reduced accidentability to unbelievable levels some decades ago. As can be seen in Table 4, two of the four riskiest points in the Western Mediterranean are situated in the south of the Iberian Peninsula, specifically in the Alboran Sea, and Arcew is on the coast of Algeria. A spill off Marseilles, the fourth area, can affect the north-east of the Iberian Peninsula. On the other hand, despite being areas of intense shipping traffic, a spill off Cape of Gata or Arcew is less likely to have a pollutant impact on the Spanish coast due to the action of sea currents.

Table 5: Approximate speed of movement of an oil slick in some Western Mediterranean areas.

Areas	Summer Oil slick direction	Winter Oil slick direction
Strait of Gibraltar	North Coast, Strait and Coast of Málaga	Coast of Málaga
Cape of Gata	Coast of Algeria	Coast of Algeria
Arcew (Algeria)	Coast of Algeria	Coast of Algeria/Open sea
Marseilles	Marseilles/Open sea	Catalan Coast/Open sea

An oil spill off Marseilles could affect the Catalan coast (NE of Spain) since the continental plateau speeds up the current. Thus, the spill would reach the coast off the Natural Park of Cape of Creus in about 2 days. The most vulnerable area is the Strait of Gibraltar. Traffic density and the high number of tankers sailing its waters and calling at the Bay of Algeciras increase the risk of accident considerably. In the event of an oil spill, the time required by the slick to reach Spain up to the coast of Malaga would be between 2 and 6 hours depending on the wind intensity.

REFERENCES

Cantano, A. (2004): El convenio MARPOL 73/78. Un estudio detallado. *MIRMAL*. Issue 14, United Kingdom.

Department of Trade (1990): *Oil Pollution Act*, Washington D.C., United States of America.

International Maritime Organisation. *International Convention on Maritime Pollution prevention. 1973*/78 as amended, London, United Kingdom.

International Maritime Organization (1996): *International Safety Management Code,* as amended, London, United Kingdom.

International Maritime Organisation: *Manual on the Pollution Occasioned by Hydrocarbons, Part IV Fighting against the Hydrocarbons Spills*. London, United Kingdom.

Feed and Agriculture Organisation, Geneve, Switzerland.

General Commission of Fishing of the Mediterranean, France.

Intergovernmental Oceanographic Commission.

International Maritime Organization (2008): *Guidance on the implementation of the LRIT system*. MSC.1/Circ.1298., 8th December 2008. London, United Kingdom.

REMPEC. (2008): *Study of Maritime Traffic Flows in the Mediterranean Sea* - Final Report, July 2008. Malta.

United Nations Conference on Trade and Development (2007) *Maritime Review*.

UN ESTUDIO DE LOS PUNTOS MÁS ARRIESGADOS DELANTE DE UNA MANCHA DE ACEITE DEBIDO A UN ACCIDENTE EN LA COSTA DEL MEDITERRÁNEO ESPAÑOL

ANEXO

El Objetivo fundamental de este artículo es el de analizar, identificar y posteriormente cuantificar, las áreas de la costa Española Mediterránea, con mayor riesgo de sufrir un derrame de hidrocarburos procedente del tráfico marítimo de hidrocarburos. En el estudio que fundamenta este artículo, se han tomado en consideración una serie de variables, de entre las que destacamos, las peculiaridades geográficas, climáticas o la densidad de tráfico, que alimenten una función aleatoria. Esta función objetiva ponderará los diferentes puntos de la costa e identificando los que tengan una mayor probabilidad de riesgo.

En la investigación aquí presentada, se pretende evidenciar dónde pueden ubicarse las áreas del Mediterráneo Occidental español donde puede haber mayor riesgo de derrame potencialmente.

En los puertos del Estrecho de Gibraltar, es donde escala el mayor número de buques tanque del sistema portuario español; alcanzando aproximadamente el 34% de las escalas, seguidos de Tarragona y Barcelona con un 20% y 16%, respectivamente. Considerando las escalas de Gibraltar, en el área del Estrecho se sobrepasaría la cifra de 4.000 al año, siendo importante reseñar que durante el año 2007 cruzaron el Estrecho de Gibraltar 105.954 buques. Según los datos del 2006, de los buques que navegan por el Estrecho de Gibraltar en tránsito hay que destacar que el 19% corresponde a buques tanque, representando el 32% del GT. El tercer factor que se estudia es la morfología del Mediterráneo Occidental. A través de las cartas náuticas obtenemos la sonda del área, asignándole un coeficiente del 0 al 10 a cada cuadrícula en función de la sonda.

Se valora también el factor de la edad de la flota. Es evidente que el riesgo de averías crece con los años y, por tanto, también el número de siniestros. En la última década, la edad de la flota se ha reducido notablemente. Otro factor importante colateral a la edad del buque es su bandera de registro. Analizando las banderas de los buques tanque, la conclusión del conjunto de los puertos ha sido que, del orden del 65% de la capacidad de carga de los buques tanques que escalan en los principales puertos del Mediterráneo Español lo hacen bajo pabellón de países occidentales, y menos de un 10% lo hace bajo pabellón de terceros países. No debemos olvidar que algunas flotas que están bajo pabellón de "conveniencia" se encuentran gestionadas por armadores de países occidentales, y que el abanderamiento se limita a una cuestión fiscal y/o de costes.

A las distintas cuadrículas del Mediterráneo Occidental se le asigna un coeficiente del 0 al 10, consecuencia del estudio de la edad de la flota y su pabellón.

Una vez analizados los cuatro factores de riesgo, procedemos al cálculo del censo de los *puntos negros*. Para ello, y tras las diferentes conclusiones obtenidas a lo largo del estudio y a la opinión de relevantes profesionales del sector, materializada a través de encuestas mandadas, le asignamos un valor porcentual a cada factor de riesgo del 60% al Tráfico, 15% al Oleaje, 10% a la Morfología, 15% a la Edad de la Flota.

Los puntos con mayor riesgo son los cuatro citados en el cuadro anterior, encontrándose tres de ellos en el sur de la Península, en las inmediaciones del mar de Alborán, y el cuarto en Marsella, pudiendo afectar a la costa Nororiental del litoral de Cataluña (Cap de Creus). De los cuatro *puntos negros* (PN) determinados, dos de ellos tienen un riesgo relativamente inferior de que la marea negra llegue al litoral español, aún cuando concentran un importante tráfico. Los PPNN de Cabo Gata y el de Arcew, tienen una probabilidad menor de impacto de la marea negra en la costa española, debido a las corriente marinas existentes.

En caso de marea negra, el PN de la zona de Marsella podría tener incidencia en el litoral de la costa catalana. Concretamente, el primer lugar donde podría impactar es en el Cap de Creus. En esa zona, la plataforma continental se hace muy estrecha, agudizándose con el Cañón de Creus, disminuyendo aún más la plataforma continental en esa área, pudiendo llegar la marea negra hasta la costa del Parque Natural de Cap de Creus. Como orden de magnitud, tenemos dos días para evitar que la marea negra pueda llegar al litoral catalán desde el PN de Marsella.

El cuarto PN y potencialmente más peligroso es el Estrecho de Gibraltar. El elevado tráfico que soporta y el gran número de buques tanque que surcan sus aguas, muchos de ellos recalando en la Bahía de Algeciras, lo convierten en el *punto negro* con mayor riesgo potencial. En caso de vertido accidental en el transporte de hidrocarburos, el efecto de la corriente y del viento haría que la costa Norte del Estrecho se viese afectada, al igual que la costa de la provincia de Málaga, desde Manilva hasta Fuengirola. Todo ello dependiendo de la época del año y de las condiciones climatológicas reinantes. Además, como orden de magnitud, el tiempo que se dispone para reaccionar es de entre dos y seis horas, en función de la época del año y la parte del litoral que se viese afectada.

INSTRUCTIONS FOR AUTHORS

http://www.jmr.unican.es

Description

Journal of Maritime Research (JMR) publishes original research papers in English analysing the maritime sector international, national, regional or local. JMR is published quarterly and the issues—whether ordinary or monographic—include both theoretical and empirical approaches to topics of current interest in line with the editorial aims and scope of the journal.

The objective of JMR is to contribute to the progress, development and diffusion of research on the maritime sector. The aim is to provide a multidisciplinary forum for studies of the sector from the perspective of all four of the following broad areas of scientific knowledge: experimental sciences, nautical sciences, engineering and social sciences.

The manuscripts presented must be unpublished works which have not been approved for publication in other journals. They must also fulfil all the requirements indicated in the 'Technical specifications' section. The quality of the papers is guaranteed by means of a process of blind review by two scientific referees and one linguistic reviewer. Although the journal is published in print format, the processes of submission and reception of manuscripts, as well as revision and correction of proofs are all done electronically.

The publication process

Submission and acceptance of manuscripts

Papers should be sent via the journal's web site at http://www.jmr.unican.es, following the guidelines indicated for the submission of manuscripts by authors. Submitting the manuscript involves sending electronically via the web site three different types of information: general information about the article and the authors, an abstract and the complete paper.

The general information about the article and the authors, as well as the acknowledgements, is to be introduced by means of an electronic form, in which the following data are requested:

- ☐ Title of the paper. Subtitle.
- ☐ Field of the manuscript presented (Experimental Sciences, Engineering, Nautical Sciences or Social Sciences) and sub-field.
- ☐ E-mail of the author to whom correspondence should be addressed.
- ☐ Personal data of each author including name, professional category or position, institution or organisation, postal address and e-mail.
- ☐ Acknowledgements, if included, should be no longer than 150 words without spaces between paragraphs.

The manuscripts submitted which are in line with the aims and scope of JMR will be submitted to a blind review process. The objective is to assess the scientific quality (two referees) and ensure that the text is linguistically acceptable (one reviewer). Only those works which are considered adequate from a scientific point of view will be reviewed linguistically. Manuscripts which do not pass the linguistic filter will be admitted with the condition that the author make linguistic and stylistic modifications as indicated.

Authors will be informed of the acceptance, rejection and/or modifications required no later than four months after the receipt of the manuscript. Once the paper has been accepted, authors can check on the status of their article via the web site. Any doubts or questions should be addressed to the Editor at jmr@unican.es

Copyright

After manuscripts have been definitively accepted, the authors must complete the copyright agreement assigning the copyright to JMR so that it can be published.

Proofs

Once the copyright transfer agreement has been completed, the Editors will assign the paper to an upcoming issue of JMR and proofs will be sent as a PDF file to the author who has corresponded with JMR throughout the reviewing process. The corrected proofs must be returned by e-mail to the Editor of JMR within 96 hours of receipt.

Reprints

Once the paper has been published, the authors will be sent a total of 12 free reprints, which will be sent the postal address of the corresponding author. Authors may also request, via the JMR web site http://www.jmr.unican.es, a maximum of 10 complete journals at 50% of the cover price.

Style and technical specifications

Manuscripts should be sent to JMR's web site in a format that is recognisable to Microsoft Word (.doc) in any of its versions for Windows. The maximum length of manuscripts is 23 double-spaced pages (approximately 7000 words) including the abstract, references and appendices. Manuscripts will be submitted using a specific application of the electronic form used to send personal data. The page layout should follow these guidelines:

- ☐ Size: DIN A4 (29 cm by 21 cm)
- ☐ Margins, 3 cm: top, bottom, left, and right.
- ☐ Font: Times New Roman, normal style, 12-point type.
- ☐ Double spacing should be used for all the paper except for the references which are to be single-spaced.
- ☐ Notes, when necessary, are to be placed at the end of the paper and numbered in their order of appearance in the text. Mathematical derivations should not be included in these endnotes.

The abstract is to be presented on one page and should include the following information:

- ☐ Title and subtitle of the paper
- ☐ Field and sub-field of the work presented.
- ☐ Abstract, which is to be no longer than 200 words, and should have no spaces between paragraphs.

- ☐ Key words (between 3 and 5) which will be used for computerised indexing of the work, in both Spanish and English.
- ☐ The complete work should be no longer than 23 pages (about 7000 words) and should be structured as is shown below.

The first page will contain the same information as the summary:

- ☐ Title of the paper, as specific and brief as possible, and subtitle if desired.
- ☐ Field and sub-field of the work presented.
- ☐ Abstract of 200 words.
- ☐ Key words.

The rest of the article:

- ☐ Introduction or Problem
- ☐ Methods
- ☐ Development (application and results)
- ☐ Conclusions
- ☐ Endnotes
- ☐ References. Only those included in the article in alphabetical order.
- ☐ Appendix containing a condensed version of the article in Spanish. This is to be 3 or at most 4 pages in length (approximately 1000-1200 words) with the following sections: abstract, methods and conclusions.

The body of the article is to be divided into sections (bold, upper-case), subsections (bold, italics) and optionally into sub-subsections (italics), none of which are to be numbered. Insert line spaces before and after the title of each section, subsection and sub-subsection. Symbols, units and other nomenclature should be in accordance with international standards.

References

The Harvard System is to be used, following the guidelines indicated below.

The way in which *bibliographic citations* are included in the text will depend on the context and the composition of the paragraph and will have one of the following forms:

- ☐ One author: Farthing (1987); (Farthing, 1987); (Farthing, 1987 pp. 182-5)
- ☐ Several authors: Goodwin and Kemp (1979); Ihere, Gorton y Sandevar (1984); Ihere et al.(1984); (Ihere et al., 1984)

The *bibliographic references* are to be arranged in alphabetical order (and chronologically in the case of several works by the same author), as is indicated in the following examples:

Books

Farthing, B. (1987) *International Shipping.* London: Lloyd´s of London Press Ltd.

Chapters of books

Bantz, C.R. (1995): Social dimensions of software development. In: Anderson, J.A. ed. *Annual review of software management and development*. Newbury Park, CA: Sage, 502-510.

Journal articles

Srivastava, S. K. and Ganapathy, C. (1997) Experimental investigations on loop-manoeuvre of underwater towed cable-array system. *Ocean Engineering* 25 (1), 85-102.

Conference papers and communications

Kroneberg, A. (1999) Preparing for the future by the use of scenarios: innovation shortsea shipping, *Proceedings of the 1st International Congress on Maritime Technological Innovations and Research,* 21-23 April, Barcelona, Spain, pp. 745-754.

Technical Reports

American Trucking Association (2000) *Motor Carrier Annual Report*. Alexandria, VA.

Doctoral theses

Aguter, A. (1995) *The linguistic significance of current British slang*. Thesis (PhD).Edinburgh University.

Patents

Philip Morris Inc., (1981). *Optical perforating apparatus and system*. European patent application 0021165 A1. 1981-01-07.

Web pages and electronic books

Holland, M. (2003). *Guide to citing Internet sources* [online]. Poole,
Bournemouth University. Available from:
http://www.bournemouth.ac.uk/library/using/guide_to_citing_internet_sourc.html
[Accessed 1 November 2003]

Electronic journals

Storchmann, K.H. (2001) The impact of fuel taxes on public transport — an empirical assessment for Germany. *Transport Policy* [online], 8 (1), pp. 19-28 . Available from:
http://www.sciencedirect.com/science/journal/0967070X
[Accessed 3 November 2003]

Equations, tables, Illustrations.

Equations are to be written with the Microsoft Word Equation Editor using right-justified alignment. They should be numbered consecutively using Arabic numerals within parentheses.

Tables should be inserted in the appropriate point in the text using Microsoft Word. They should be numbered consecutively with Arabic numerals and a concise title should be centred at the top of the table. The source is to be indicated at the bottom on the left. Any symbols used should be explained.

Illustrations are to be inserted in the appropriate point in the text using Microsoft Word. All illustrations (graphs, diagrams, sketches, photographs, etc.) will be denominated generically Figures and are to be numbered consecutively using Arabic numerals with the title centred at the top. The source is to be indicated at the bottom on the left. Photographs must be in black and white with a quality of at least 300 ppp.